

# CO-EFFICIENT OF ROLLING RESISTANCE OF ELASTIC WHEELS ON A FLAT SURFACE

A Thesis Submitted  
In Partial Fulfilment of the Requirements  
for the Degree of  
MASTER OF TECHNOLOGY

*by*

VENKATA SUBBA RAO KOMARAGIRI

*to the*

DEPARTMENT OF MECHANICAL ENGINEERING  
INDIAN INSTITUTE OF TECHNOLOGY, KANPUR  
FEBRUARY, 1984

ME-1984-M-KOM-CO-EFF

CERTIFICATE

This is to certify that this thesis entitled,  
" CO-EFFICIENT OF ROLLING RESISTANCE OF ELASTIC WHEELS  
ON A FLAT SURFACE" , submitted in partial fulfilment of  
the requirements for the Degree of Master of Technology  
by Mr. VENKATA SUBBA RAO KOMARAGIRI, is a record of work  
carried out under my supervision and has not been submitted  
elsewhere for a degree.

*Prashant Kumar*

February, 1984

DR. PRASHANT KUMAR  
ASSISTANT PROFESSOR  
DEPT. OF MECHANICAL ENGINEERING  
INDIAN INSTITUTE OF TECHNOLOGY  
KANPUR-208016, INDIA

### ACKNOWLEDGEMENT

I express my deep sense of gratitude and appreciation to Dr. Prashant Kumar, Asst. Professor, Department of Mechanical Engineering, I.I.T., Kanpur, India, for suggesting this problem, his constant inspiration, invaluable suggestions and constructive criticism throughout the duration of my thesis work.

My thanks are due to Prof. B.D. Agarwal of the same department for his helping hand at times. My thanks are also due to Mr. G.N.M. Sudhakar, R.E., Electrical Engg. Dept. for his invaluable help in setting up photo-diode arrangement for the measurement of velocity. My sincere thanks are due to Mr. Ch. L.V. Ramana Rao, M. Tech. (Civil) for his timely help on several occasions during my thesis work, Mr. R. Venugopal, M. Tech. (NET), Mr. K. Sarat Babu M. Tech. (Mech.), Mr. Y.V. Srinivas M. Tech. (CS), Mr. T.S. Vasishta and other well-wishers who gave me constant encouragement throughout this period.

I am highly grateful to Mr. R.S. Shukla, Mr. S.N. Dwivedi and Mr. S. Viswakarma, for their helping hand in performing this experiment. I appreciate Mr. S.L. Srivastava,

20152

Mr. D.K. Sarkar and Mr. S.N. Yadav for their willingness at any time to help me during my work.

I also thank Mr. D.P. Saini for his flawless typing, Mr. Ayodhya Prasad for cyclostyling and Mr. Gauri Singh for tracings.

(SUBBA RAO)

CONTENTS

	<u>Page</u>
LIST OF FIGURES	v
LIST OF TABLES	vii
LIST OF SYMBOLS	viii
ABSTRACT	ix
CHAPTER-I : INTRODUCTION	1
CHAPTER-II : MECHANISMS OF ENERGY LOSSES DURING ROLLING	10
CHAPTER-III : THEORETICAL DEVELOPMENT	13
CHAPTER-IV : EXPERIMENTAL ARRANGEMENT	34
CHAPTER-V : EXPERIMENTAL RESULTS AND DISCUSSIONS	48
CHAPTER-VI : CONCLUSIONS , SCOPE AND FURTHER STUDY	65
REFERENCES :	68

# LIST OF FIGURES

	Page
Fig. 1(a) Rolling of a wheel on a flat surface	
(b) Details of Sector $S_1$ .	15
Fig. 2 Two wheels in contact.	18
Fig. 3 Theoretical curves for $\mu$ vs $Q$ under plane stress and plane strain conditions - ordinary scale	30
Fig. 4 Theoretical curves for $\mu$ vs $Q$ under plane stress and plane strain conditions - semi-log scale	31
Fig. 5 Schematic diagram of the experimental arrangement	35
Fig. 6 Overall view of wheel rolling experimental set-up	37a
Fig. 7 Close- view of the plexi-glass wheel attached with disk shaped Aluminium weights	37b
Fig. 8 Stress-strain curve for plexi-glass material under compression	38
Fig. 9 Stress-strain curve for Teflon material under compression	39
Fig.10 Close view of the rolling surface of grooved Teflon wheel	40
Fig.11 Close view of the photo-diode arrangement.	43
Fig.12 Circuit diagram for photo diode arrangement:	44
(a) circuit diagram for bulbs	
(b) circuit diagram for photo-diode	

	<u>Page</u>
Fig.13 $\mu$ vs $Q$ for plexi-glass wheels rolling on plexi-glass flat surface - on ordinary scale	49
Fig.14 $\mu$ vs $Q$ for plexi-glass wheel rolling on plexi-glass flat surface - on semi-log scale	50
Fig.15      Comparison of the results of present study with the work of Hasnain	52
Fig.16 $\mu$ vs $Q$ for Teflon wheels rolling on a plexi-glass flat surface - on ordinary scale	55
Fig.17 $\mu$ vs $Q$ for Teflon wheels rolling on a plexi-glass flat surface - on semi-log scale	56
Fig.18      Overall graph of $\mu$ vs $Q$ on ordinary scale	58
Fig.19      Overall graph of $\mu$ vs $Q$ on semi-log scale	59



LIST OF TABLES

Table 1	: Geometric parameters, material constants and Chakra No. for different wheels.	60
Table 2	: Co-efficient of rolling resistance $\mu$ for plexi-glass wheels rolling on a plexi-glass flat surface	61
Table 3	: Co-efficient of rolling resistance $\mu$ for Teflon wheels rolling on a plexi-glass flat surface	62
Table 4	: (a) Sample calculations for wheel No. 5, set No. 16	63
	(b) Sample calculations for wheel No. 6, set No. 24	64

LIST OF SYMBOLS

	<u>DESCRIPTION</u>	<u>SYMBOL</u>
1.	Normal load per unit contact width of a wheel	N
2.	Radius of wheel	R
3.	Young's modulus of elasticity for the material of wheel	$E_1$
4.	Young's modulus of elasticity for the material of flat surface	$E_2$
5.	Equivalent Young's modulus	E
6.	Strain energy	U
7.	Force per unit width to overcome the rolling resistance	F
8.	Linear velocity of centre of the wheel	V
9.	Stress at a point	$\sigma$
10.	Strain at a point	$\epsilon$
11.	Chakra Number (N/ER)	$\Omega$
12.	Co-efficient of rolling resistance	$\mu$
13.	Half-contact length between the wheel and the flat surface	$a_0$
14.	Poisson's ratio	$\nu$
15.	Linear acceleration of the wheel	a
16.	Angular acceleration of the wheel	$\alpha$
17.	Radius of gyration of the wheel	k

### ABSTRACT

The various mechanisms responsible for energy losses during rolling of a wheel under elastic conditions are presented. A theoretical formulation based on the strain energy release is presented to determine the energy losses of a slow rolling wheel under elastic conditions and it predicts that the overall co-efficient of rolling resistance,  $\mu$ , is proportional to the square root of a dimensionless number, called 'Chakra Number',  $Q$  ( $Q = \frac{N}{ER}$ ), where  $N$  is the normal load per unit width of the wheel,  $R$  is the radius of the wheel and  $E$  is the equivalent Young's modulus of the materials of wheel and the flat surface. The co-efficient of rolling resistance,  $\mu$ , comes out to be 15.48% greater for plane stress over plane strain condition.

To obtain the experimental data, a suitable experimental set-up is devised by rolling a wheel, made of plexi-glass or Teflon on a smooth flat strip of plexi-glass. The rolling is carried out at speeds of 0.06 - 0.15 m/sec. and an initial velocity is given by a suitably designed ramp placed at one end of the rolling

strip. The retardation of the motion of the wheel is measured using photo-diode arrangements located at three stations.

The experiments are conducted by varying the load per unit thickness ( $N$ ), thus obtaining  $\mu$  between 0.0014 and 0.0053. The experimental results of plexi-glass wheels are closer to plane stress predictions and results of Teflon wheels are in good agreement with the plane strain predictions.

## CHAPTER-I

### INTRODUCTION

It is estimated that one-third of the world's total energy is lost in friction. In some applications, we want high friction. For instance, when we walk on roads, high friction prevents slipping. In some applications, we want friction to be as small as possible such as in machine parts, for smooth operation and long life. The principle of rolling through circular objects, such as, wheels or logs have been used by man since prehistoric time. As prehistoric times experience says, it is true even today, that rolling friction is much less than sliding friction. When one object roll's over another, the molecular bonds are broken by a 'lifting motion' where as a sliding motion requires a 'shearing effect'.

The study of energy losses in the rolling did not begin until the late eighteenth century. The first systematic study was undertaken by Coulomb [1] in 1785. By pulling wooden cylindrical wheels over flat wooden surfaces, he found that the pulling force needed to overcome rolling resistance is directly proportional to the

normal load, and inversely proportional to the wheel radius. However, coulomb and his contemporaries did not employ energy concepts in their analyses. In fact, wheels were assumed to be rigid by coulomb; rolling losses were due to vibrations generated in the bodies because of the irregularities on the rolling surface and also due to the deformation of the surface. Although coulomb remarked that the linear dependence of rolling friction is similar to that observed in ordinary sliding friction, he did not express any explicit view about the basic mechanism of the rolling friction. Nevertheless, coulomb established that the pulling force  $F$  to overcome the rolling resistance is equal to  $\frac{eN}{R}$ , where  $N$  is the normal load on the wheel,  $R$  its radius and  $e$  is the proportionality constant or a parameter which depends on the properties of materials used. Although, this formulation of coulomb has been quite popular among the designers through ages, the relation is empirical as one has to evaluate the proportionality constant 'e' through experiments. Other investigators[2] claim that the proportionality constant 'e' is proportional to the square root of the wheel radius, and therefore, the pulling force  $F$  is proportional to  $\frac{N}{\sqrt{R}}$ .

The next contribution in this direction was made almost a century afterwards, by Osborne Reynolds [3] in 1876. His empirical observations agreed with those of

coulomb. In addition, he proposed an explicit theory of rolling friction attributing the rolling resistance to cause essentially the same as those responsible for ordinary sliding friction. It was to imply this connection that he deliberately used the term 'rolling-friction' instead of 'rolling resistance'. Reynolds observed that when a metal cylinder rolls over a flat rubber surface, it moves forward, in each revolution, a distance less than the circumference of the cylinder. From his earlier work on the slip of the leather belts over cylindrical pulleys, Reynolds concluded that there was a similar kind of slipping between the roller and the rubber surface. Within the region of contact, different elements of the rubber surface are stretched, elastically, by different amounts: this differential elastic stretching leads to microslip within the contact region with corresponding dissipation of frictional energy. Reynolds also observed that the cylinder tended to oscillate whenever it was slightly disturbed from rest on the rubber surface and realized that this involved something more than interfacial slip. He pointed out that "these oscillations could not have been caused by the mere resistance which the one surface offered to the sliding of the other over it, unless also this resistance threw the surfaces into constraint from which they were constantly endeavouring to free themselves".

Another contribution of considerable importance is that of Heathcote[4] in 1921, who pointed out that when the rolling element is a sphere, instead of a cylinder, there is far more important source of interfacial slip than that proposed by Reynolds. When sphere rolls in a groove, different parts of the region of contact are at different distances from the axis of rotation of the sphere. Consequently, they measure out different distances for each revolution of the sphere, and this in turn produces differential slip between the ball and the ellipse of contact. This suggestion was supported by the damage produced in the groove after prolonged running, but no quantitative estimate was made of the magnitude of the rolling friction to be expected from this type of differential slip.

Tomlinson [5] in 1929, described some very careful experiments on the rolling of metallic cylinders at relatively light loads, and came to the conclusion that the differential stretching described by Reynolds would be far too small to account for the rolling resistance. Further in his own experiments, he would have expected the Reynolds type of microslip to produce fretting corrosion, but no such corrosion was observed. Tomlinson explained his observations in terms of molecular adhesion between the rolling surfaces arising from short



range interfacial forces. As the rolling elements roll apart, the surface atoms are pulled away from their equilibrium positions until the displacement exceeds a certain distance, they then 'flick' back to their old equilibrium positions, and, in the process, energy equivalent to the rolling frictional loss is dissipated. In his experiments Tomlinson performed a metal ball to roll over another metal ball of the same material and of the same diameter, so that, the surface of contact must by symmetry, be plane consequently, no differential slip of Heathcote type can occur. Further, any lateral extension or compression of the surfaces at the interface will be identical for both spheres so that no slip of Reynolds type will occur. In spite of taking care of these two effects, he observed appreciable amount of rolling friction.

It is seen that the above three major contributions to the mechanism of rolling friction involve same type of interfacial friction or surface interaction. For this reason, they all face a very serious difficulty that over a wide range of experimental conditions, lubricants have little effect on the magnitude of the rolling resistance.

Later on in 1955, Tabor [6] conducted an experiment in which a steel cylinder of 1/2 inch diameter was

supported on two small ball-races and rolled over a rectangular block of red bung rubber. Under heavy loads producing large deformations, it was found that in a single revolution of the cylinder the distance travelled forward was 10% less than the circumference of the cylinder, since the arc of contact was approximately 1 cm ( $\approx \frac{1}{2}$ ") overall slip might be about 1 mm (= 10%). To see whether this was so, a small hole 1 mm in dia was drilled diametrically through the roller and its edges were painted with painter's ink so that it could form an impression on the rubber. Under static loading a clear circular imprint was formed and during rolling an equally sharp imprint was formed without any trace of blurring or smearing of the outline. However, the imprint was elliptical with the minor axis 10% smaller than the major axis. From this he made two conclusions ; (i) the discrepancy between the circumference and the distance travelled does not correspond to the gross slip at the rolling interface. The rubber is stretched before it enters and after it leaves the region of contact and the cylinder merely measures out its periphery on rubber that is stretched by 10% , (ii) Reynolds suggested that the stretching of an element of the rubber at different points of contact region may be different so that there would be a second order slip between those points to accommodate the change in stretching. The

sharpness of the imprint shows that this slipping, if it does occur, is of negligible and quite insufficient to account for the observed rolling friction. Thus according to Tabor the resistance to rolling is not primarily the result of interfacial slip. Nor can it be due to interfacial adhesion, since the experiments show that when the surfaces are lubricated with glycerine, the rolling friction is not substantially changed. So according to him the only source of energy loss is elastic hysteresis.

However, utilization of the mechanism of energy dissipation to calculate the rolling losses has been carried out first time by Holt and Wormeley [7] in 1922 earlier to Taber [6]. They developed an experimental method to evaluate rolling losses in automobile tyres. In this method, tyres were rolled on a drum revolving on a fixed axis. The power input to the tyre and the power output from the drum were measured. The difference in the two values provided the losses in the tyre.

Tabor [6] in 1955 and Drutowski [8] in 1959 analysed the losses of a ball rolling on a flat surface. They argued that due to cyclic loading and hysteresis effect, energy is continuously lost and hence a force is needed to keep the ball rolling. But in elastic materials, such as steel, hysteresis losses are negligible

especially when the load on a ball is small enough and the contact stresses are smaller than yield stresses. Rolling losses are known to be appreciable even for low stresses and therefore a mechanism is needed to explain this behaviour.

Greenwood, Minshall and Tabor [9] explained the rolling losses in terms of frictional torque acting on a rolling body. According to their model, the difference in pressure acting on the front half of the contact area from that on the rear half of a rolling wheel applies a torque on the body. The product of the torque and the angular velocity provides the energy loss. They claim that the analysis is based on energy principle, but it is actually based on force analysis to evaluate the frictional torque. As a matter of fact, due to approximately symmetric pressure distribution in the contact area, net torque on the freely moving wheel is small compared with the torque exerted by either half.

Thus, there appears to be lack of clear understanding concerning physical mechanisms responsible for energy losses during rolling, and, consequently missing is a plausible theoretical formulation determining rolling losses. Recently, Hasnain [10] developed a model, using strain-energy release mechanism, in which, coefficient of rolling resistance of a wheel is proportional

to a dimensionless group ( $N/ER$ ), when it is rolled on a flat surface. Where  $N$  is the load per unit thickness of wheel,  $E$ , equivalent Young's modulus and  $R$ , radius of the wheel. The present experimental investigation is for verifying this model.

This study names the various mechanisms causing rolling losses and discusses briefly some of them in Chapter-II, while a theoretical development is presented in Chapter-III to determine the energy losses of a slow moving wheel over a flat surface under elastic conditions. Chapter-IV describes the experimental arrangement devised to verify the analytical results whereas, experimental results and discussions are presented in Chapter-V. Chapter-VI is devoted for the conclusions, scope and further study.

## CHAPTER-II

### MECHANISMS OF ENERGY LOSSES DURING ROLLING

Following mechanisms are the primary mechanisms for the rolling losses in general:

(i) Strain Energy Release:

When a wheel rolls, material adjacent to the contact area is compressed producing stresses in the wheel and the surface on which the wheel is rolled. As rolling progresses the contact area shifts and energy stored in the material due to contact stresses is released through stress waves propagating in the wheel as well as in the surface. In the wheel the stress waves propagate in all directions. When the stress waves reach free surfaces, energy propagates further through surface waves and reflected body waves into the wheel. Further, these stress waves interact with numerous imperfections such as point defects like impurity atoms, line defects such as dislocations etc. Consequently, by the time wheel makes a full round and the same portion of the wheel is about to be compressed, major portion of the strain energy is converted into heat. Because of the compression between the wheel

and the flat surface energy is lost continuously and it has to be supplied by an external force to keep the wheel rolling at a constant velocity.

(ii) Vibrations due to Roughness of Surfaces:

Influence of surface roughness during rolling is analogous to a wheel rolling over a stone or a protrusion on a flat surface. When the wheel jumps over it, vibrations are produced. The energy in the form of vibrations is no longer useful to roll the wheel forward. Kinetic and strain energies of these vibrations are also eventually converted to heat energy through dissipation at imperfections in the materials. The mechanism is not significant when the rolling surfaces are smooth. It becomes important only when the surfaces are uneven.

(iii) Sliding of Contact Surfaces:

In an ideal case of a rigid wheel rolling over a rigid flat surface contact occurs on a line. However, due to deformation of the rolling bodies, the contact occurs on a rectangular area. Theoretically the portion of the wheel in contact with the stationary flat surface should have zero velocity, but the moving wheel tends to make its rolling surface move at the contact area. This may cause sliding within the contact area and therefore,

energy loss occurs. Its effect may be significant if the length of the contact area is large in comparison to the radius of the wheel.

(iv) Impact on Flat Surface:

In an ideal case of a rigid wheel rolling over a rigid stationary flat surface the velocity at the contact point is essentially zero. But in deformable bodies, a segment of the rolling surface about to touch the stationary flat surface has a non-zero velocity thus causing impact. These losses are more at higher velocities and loads.

(v) If the load is high enough to cause yielding in both the materials, plastic flow takes place consequently causing a loss of energy.

Thus, the major parameters responsible for rolling losses are:

- (a) Moduli of the wheel and the flat surface
- (b) Surface roughness of wheel and the flat surface
- (c) Material properties of wheel and the flat surface such as yield stress, work hardening etc.
- (d) Pattern on the rolling surfaces such as, treads on pneumatic tyres
- (e) Velocity of the wheel
- (f) Width of the wheel
- (g) Diameter of the wheel
- (h) Load on the wheel.



### CHAPTER-III

#### THEORETICAL DEVELOPMENT

This study [10] deals only with the first mechanism of losses during rolling of a disc-shaped wheel, where, the losses are due to release of strain energy as described in Chapter-II. In order to minimize other losses, care has been taken. For example, to reduce impact losses, velocities of the wheel are kept small enough to cause 'quasi-static' deformation and the loads applied on the wheel are low enough to ensure that the stresses developed be well below the elastic limit. To reduce the effect of surface roughness and irregularities, materials which have smooth rolling surface are considered.

#### (A) Analysis of Strain Energy Mechanism During Rolling:

This analysis is based on two points :

- (a) considering the flat surface as the cylinder of infinite radius, we can calculate the stresses at the contact point between the wheel and the flat surface,
- (b) finding the stresses both at the contact point diametrically opposite point on the wheel, we can findout the strain energy loss in the wheel.

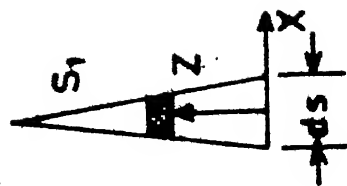
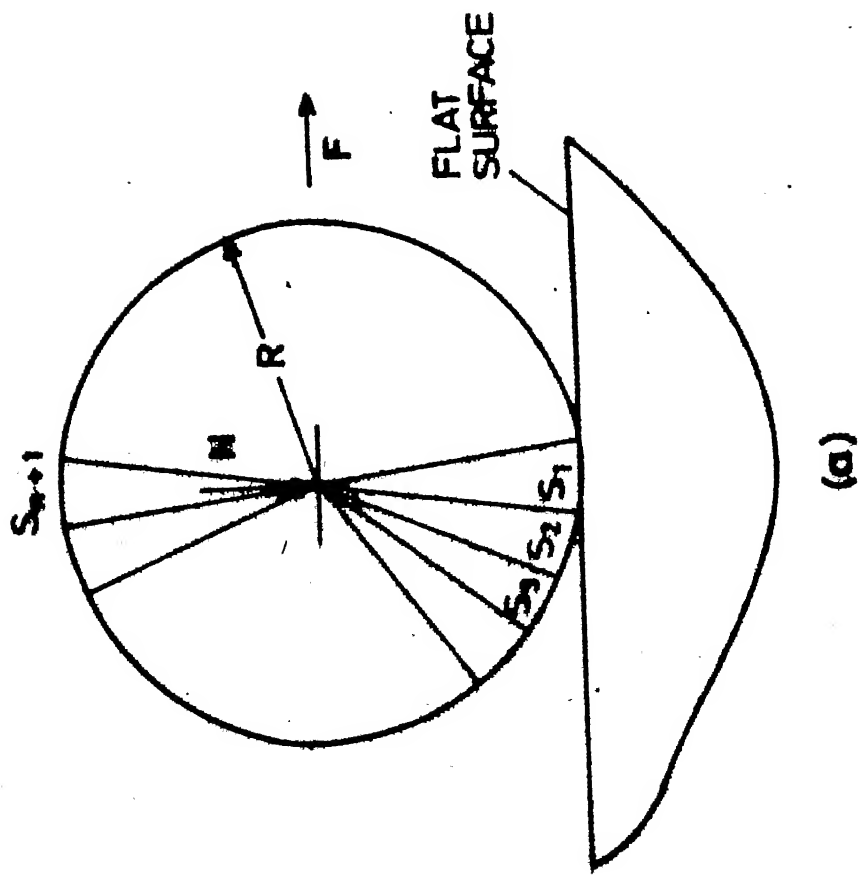
Further, as flat surface is nothing but a wheel of infinite radius, we can determine its strain energy losses by using the same formula. Then using the overall strain energy loss and employing elementary dynamics we can find out the co-efficient of rolling resistance  $\mu$ .

As discussed by Hasnain [10], consider, a wheel of uniform width [Fig.1(a)], divided into a large number  $(2n)$  of identical sectors. The load per unit width (width, which is in contact with the flat surface) on the wheel is denoted by  $N$  and the force per unit width needed to keep the wheel rolling at constant velocity is denoted by  $F$ . The sector  $S_1$  is stressed the most. When the sector  $S_1$  moves to the position of  $S_2$ , strain energy is released in the form of stress waves. At the same time, the sector  $S_2$ , releases a part of its strain energy, as it moves to the position of sector  $S_3$ . Therefore the total strain energy release  $\Delta u$ , is given by

$$\begin{aligned}\Delta u &= (u_1 - u_2) + (u_2 - u_3) + \dots + (u_n - u_{n+1}) \\ &= (u_1 - u_{n+1})\end{aligned}$$

Where,  $u_1$  is the strain energy of sector  $S_1$ . If  $\Delta t$  is the time taken by sector  $S_1$  to move to the position of  $S_2$ , the power  $P$ , consumed by the wheel is

$$P = \frac{u_1 - u_{n+1}}{\Delta t}$$



Details of sector  $S_1$

Fig.1 Rolling of a wheel on a flat surfaces.

Since  $\Delta t = ds/V$ ,

$$P = \frac{u_1 - u_{n+1}}{ds} V \quad (1)$$

Where  $V$  is the velocity of the centre of the wheel and  $ds$  is the length of the arc on the sector of a rolling wheel as shown in Fig. 1(b). Strain energy  $u_1$ , for a sector is given by,

$$u_1 = \int_0^R \frac{1}{2} \sigma_{kl} \varepsilon_{kl} \left(1 - \frac{Z}{R}\right) ds dZ$$

Where,  $\sigma_{kl}$  and  $\varepsilon_{kl}$  are stresses and strains at a point, and  $R$  is the radius of the wheel. If strain energy  $u_1$  is expressed by the relation,  $u_1 = \phi_1 ds$ , where  $\phi_1$  is defined by

$$\phi_1 = \int_0^R \frac{1}{2} \sigma_{kl} \varepsilon_{kl} \left(1 - \frac{Z}{R}\right) dZ \quad (2)$$

then eqn. (1) becomes

$$P = (\phi_1 - \phi_{n+1}) V \quad (3)$$

Since, this equation of power consumption is independent of the number of sectors,  $n$  can tend to infinity. Then  $\phi_1$  and  $\phi_{n+1}$  are expressed only in terms of stresses and strains on a plane passing through the centre of the contact area to the axis of the wheel. This helps in calculations, as it is no longer required to know the stress distribution within the whole of the body.

In the front half of the wheel, strain energy in a sector increases as it rotates towards the flat surface. The external force  $F$  works to increase strain energy of sectors in front half of the wheel while in the rear half of the wheel, strain energy is released in the form of heat.

The co-efficient of rolling resistance,  $\mu$ , is commonly defined by

$$F = \mu N \quad \dots \quad (4)$$

The product of force  $F$  and wheel velocity  $V$  gives the power consumption,

$$P = \mu N V \quad \dots \quad (5)$$

comparison of equns. (3) and (5) results into the equation

$$\mu_1 = (\phi_1 - \phi_{n+1})/N \quad (6)$$

Where,  $\mu_1$  amounts for the energy loss in the body of the wheel. A similar energy loss occurs in the body of the flat surface, which can be denoted by  $\mu_2$ . Therefore the overall co-efficient of rolling resistance is

$$\mu = \mu_1 + \mu_2 \quad (7)$$

For the evaluation of  $\phi_1$ , stress distribution on the radial plane of sector  $S_1$  is taken from the work of Smith and Liu [11]. In a general case of a cylindrical wheel rolling over another cylindrical surface [Fig.2],

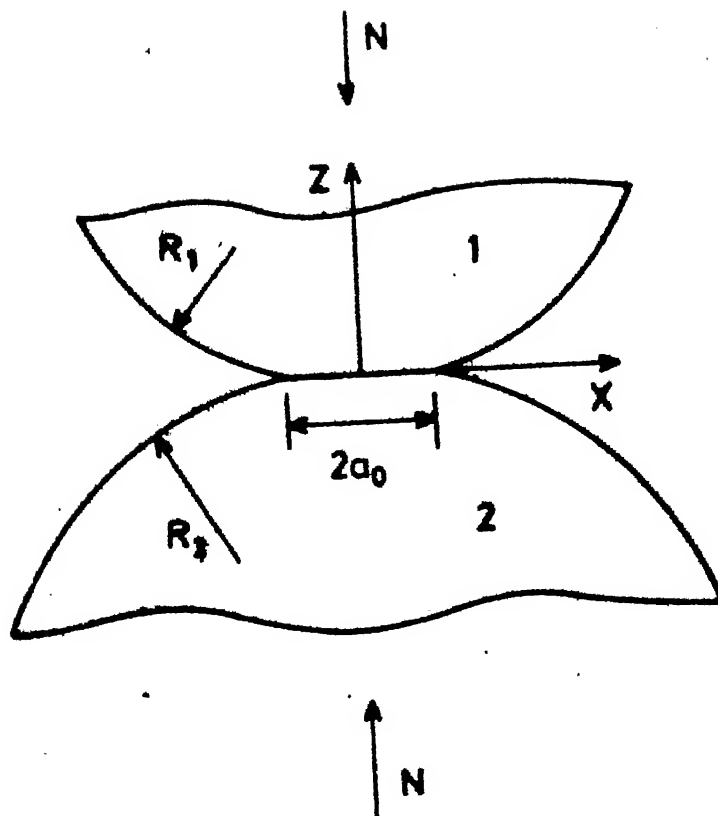


Fig.2 Two wheels in contact.

the maximum pressure at the contact area is given by,

$$p_o = \frac{2N}{\pi a_o} \quad \dots \quad (8)$$

Where,  $a_o = (\frac{2N\Delta}{\pi})^{1/2}$  = half the contact length

$$\text{and} \quad \Delta = \frac{1}{\frac{1}{2} \left( \frac{1}{R_1} + \frac{1}{R_2} \right)} \left[ \frac{1-\nu_1^2}{E_1} + \frac{1-\nu_2^2}{E_2} \right] \quad (9)$$

Here,  $E_i$ ,  $\nu_i$  and  $R_i$  are the Young's modulus, Poisson's ratio and radius of the wheel respectively. In the case of a wheel rolling over a flat surface, shear stresses are zero on the plane  $X = 0$  due to symmetric loading and the two normal stress components in the wheel are

$$\sigma_{xx} = \frac{p_o}{a_o} \left[ 2Z - \frac{a_o^2 + 2Z^2}{(a_o^2 + Z^2)^{1/2}} \right] \quad (10)$$

$$\text{and} \quad \sigma_{zz} = - \frac{p_o a_o}{(a_o^2 + Z^2)^{1/2}} \quad (11)$$

Stresses in the wheel body by eqns. 10 and 11 are same for both cases of plane stress and plane strain. However, the third normal component  $\sigma_{yy}$  will be zero for plane stress situation and for plane strain situation it is given by [11] ,

$$\sigma_{yy} = \nu_i (\sigma_{xx} + \sigma_{zz})$$

(B) Plane Stress Problem :

For a wheel of small width, the wheel deforms elastically in plane stress with the principal stress components  $\sigma_{xx}$  and  $\sigma_{zz}$  given by eqns. 10 and 11 being the only non-zero components and  $\sigma_{xz} = 0$ . Then, for sector  $S_1$ ,

$$\phi_1 = \frac{1}{2} \int_0^R \sigma_{kl} \epsilon_{kl} \left(1 - \frac{Z}{R}\right) dZ \quad (12)$$

where,

$$\begin{aligned} \sigma_{kl} \epsilon_{kl} &= \sigma_{xx} \epsilon_{xx} + \sigma_{zz} \epsilon_{zz} \\ &= \sigma_{xx} \cdot \left( \frac{\sigma_{xx} - \nu_1 \sigma_{zz}}{E_1} \right) \\ &\quad + \sigma_{zz} \cdot \left( \frac{\sigma_{zz} - \nu_1 \sigma_{xx}}{E_1} \right) \\ &= \frac{\sigma_{xx}^2}{E_1} + \frac{\sigma_{zz}^2}{E_1} - \frac{2\nu_1}{E_1} \cdot \sigma_{xx} \cdot \sigma_{zz} \end{aligned} \quad (13)$$

By substituting eqn. (13) in eqn. (12), one obtains,

$$\phi_1 = \frac{1}{2E_1} \cdot I_1 + \frac{1}{2E_1} \cdot I_2 - \frac{\nu_1}{E_1} \cdot I_3 \quad (14)$$

where,

$$I_1 = \int_0^R \sigma_{xx}^2 \left(1 - \frac{Z}{R}\right) dZ \quad (15)$$

$$I_2 = \int_0^R \sigma_{zz}^2 \left(1 - \frac{Z}{R}\right) dZ \quad (16)$$

and  $I_3 = \int_0^R \sigma_{xx} \sigma_{zz} \left(1 - \frac{Z}{R}\right) dZ \quad (17)$



(C) Plane Strain Problem :

If width of the wheel is large, the wheel deforms elastically in plane strain and then for sector  $S_1$ ,

$$\phi_1 = \frac{1}{2} \int_0^R \sigma_{kl} \varepsilon_{kl} \left(1 - \frac{Z}{R}\right) dZ$$

where

$$\begin{aligned} \sigma_{kl} \varepsilon_{kl} &= \frac{\sigma_{xx}}{E_1} \left[ \sigma_{xx} - \nu_1 (\sigma_{yy} + \sigma_{zz}) \right] \\ &+ \frac{\sigma_{zz}}{E_1} \left[ \sigma_{zz} - \nu_1 (\sigma_{xx} + \sigma_{yy}) \right] \\ &= \left( \frac{1-\nu_1^2}{E_1} \right) \sigma_{xx}^2 + \left( \frac{1-\nu_1^2}{E_2} \right) \sigma_{zz}^2 \\ &- \frac{2\nu_1}{E_1} (1+\nu_1) \sigma_{xx} \sigma_{zz} \end{aligned} \quad (18)$$

Therefore  $\phi_1$  becomes,

$$\begin{aligned} \phi_1 &= \left( \frac{1-\nu_1^2}{2E_1} \right) \int_0^R \sigma_{xx}^2 \left(1 - \frac{Z}{R}\right) dZ \\ &+ \left( \frac{1-\nu_1^2}{2E_1} \right) \int_0^R \sigma_{zz}^2 \left(1 - \frac{Z}{R}\right) dZ \\ &- \frac{\nu_1}{E_1} (1 + \nu_1) \int_0^R \sigma_{xx} \sigma_{zz} \left(1 - \frac{Z}{R}\right) dZ \\ \therefore \phi_1 &= \left( \frac{1-\nu_1^2}{2E_1} \right) \cdot I_1 + \left( \frac{1-\nu_1^2}{2E_1} \right) I_2 - \frac{\nu_1}{E_1} (1 + \nu_1) \cdot I_3 \\ &\dots \quad (19) \end{aligned}$$

In order to solve for the values of  $\phi_1$  for both the cases of plane stress and plane strain, the integrals  $I_1$ ,  $I_2$  and  $I_3$  are evaluated in the next section.

(D) Evaluation of Integrals:

Substitution of  $\sigma_{xx}$  and  $\sigma_{zz}$  from the eqns. 10 and 11 in the formulae for  $I_1$ ,  $I_2$  and  $I_3$  and carrying out the integration one can obtain

$$\begin{aligned}
 I_1 = & p_o^2 a_o \left[ \tan^{-1}\left(\frac{R}{a_o}\right) - \frac{4}{3} \right] + p_o^2 R \left[ \left(1 + \frac{1}{2} \frac{a_o^2}{R^2} \right. \right. \\
 & \left. \left. - \frac{1}{8} \cdot \frac{a_o^4}{R^4} + \frac{1}{16} \frac{a_o^6}{R^6} - \dots \right) \right. \\
 & \left. - \left(1 + \frac{1}{4} \frac{a_o^2}{R^2} - \frac{1}{24} \frac{a_o^4}{R^4} + \frac{1}{64} \frac{a_o^6}{R^6} - \dots \right) \right] \\
 & + \frac{p_o^2 a_o^2}{R} \ln \left[ 1 + \frac{1}{\left(1 + \frac{a_o^2}{R^2}\right)^{1/2}} \right]
 \end{aligned}$$

noting that for small values of  $(a_o/R)$ ,  $\tan^{-1}(R/a_o) = (\frac{\pi}{2} - \frac{a_o}{R})$  and higher powers of  $a_o/R$  can be neglected,

$$I_1 = p_o^2 a_o \left[ \frac{\pi}{2} - \frac{a_o}{R} - \frac{4}{3} + \frac{1}{4} \frac{a_o}{R} \right] + \frac{p_o^2 a_o^2}{R} \ln 2$$

$$\therefore I_1 = p_o^2 a_o \left[ 0.2375 - 0.05635 \left( \frac{a_o}{R} \right) \right] \quad (20)$$

$$I_2 = p_o^2 a_o \left[ \left( \frac{\pi}{2} - \frac{a_o}{R} \right) + \frac{a_o}{R} \ln \left( \frac{a_o}{R} \right) \right] \quad (21)$$

$$\begin{aligned}
 I_3 = & p_o^2 \left[ -a_o \cdot \tan^{-1}\left(\frac{R}{a_o}\right) \right. \\
 & \left. - a_o \left( \frac{a_o}{2R} - \frac{1}{8} \frac{a_o^3}{R^3} + \frac{1}{16} \frac{a_o^5}{R^5} - 2 \right) \right] \\
 & + p_o^2 \left[ \frac{a_o^2}{R} \ln \left( \frac{R}{a_o} \right) - \frac{a_o^2}{R} \ln \left( \frac{R + \sqrt{a_o^2 + R^2}}{a_o} \right) \right]
 \end{aligned}$$

as  $a_o \leq R$ ,  $\tan^{-1} (R/a_o) = (\pi/2 - a_o/R)$

$$\text{and } \ln \left( \frac{R}{a_o} + \sqrt{a_o^2 + R^2} / a_o \right) = \ln (2R/a_o) \\ = \ln 2 - \ln (a_o/R)$$

By neglecting the higher powers of  $(a_o/R)$ , we have

$$I_3 = p_o^2 a_o \left[ -\frac{\pi}{2} + 2 + \frac{a_o}{2R} - \frac{a_o}{R} \ln 2 + \left(\frac{a_o}{R}\right) \cdot \ln\left(\frac{a_o}{R}\right) \right] \\ = p_o^2 a_o \left[ 0.4292 - 0.1931 \left(\frac{a_o}{R}\right) + \left(\frac{a_o}{R}\right) \cdot \ln\left(\frac{a_o}{R}\right) \right] \\ \dots \quad (22)$$

(E) Analytical Results and Discussions:

(a) Plane stress case : Substituting the values of integrals  $I_1$ ,  $I_2$  and  $I_3$  in the expression for  $\phi_1$  of eqn. 14 yields

$$\phi_1 = \frac{p_o^2 a_o}{2E_1} [0.2375 - 0.05685 (a_o/R)] \\ + \frac{p_o^2 a_o}{2E_1} \left[ \left(\frac{\pi}{2} - \frac{a_o}{R}\right) + \left(\frac{a_o}{R}\right) \cdot \ln\left(\frac{a_o}{R}\right) \right] \\ - \frac{v_1}{E_1} p_o^2 a_o \left[ 0.4292 - 0.1931 \left(\frac{a_o}{R}\right) + \left(\frac{a_o}{R}\right) \cdot \ln\left(\frac{a_o}{R}\right) \right] \\ = \frac{p_o^2 a_o}{E_1} \left[ 0.9041 - 0.4292 v_1 + \left(\frac{a_o}{R}\right) \times \right. \\ \left. \left\{ 0.1931 v_1 - 0.5285 + (0.5 - v_1) \ln\left(\frac{a_o}{R}\right) \right\} \right] \\ \dots \quad (23)$$

As  $(a_o/R)$  is usually very small (of the order of 0.025), neglecting the terms containing  $(a_o/R)$  in the above eqn., we have

$$\phi_1 = \frac{p_o^2 a_o}{E_1} [0.9041 - 0.4292 v_1] \quad (24)$$

Since the load  $N$  acts at the centre of the wheel, portion of the wheel-half diametrically opposite to the contact point is very lightly loaded. Therefore,  $\phi_{n+1}$  in sector  $S_{n+1}$  is negligible in comparison to  $\phi_1$ .

Thus from eqn. 6, the co-efficient of rolling resistance for the wheel is

$$\mu = \frac{\phi_1}{N} \quad \dots \quad (25)$$

The energy loss in the flat surface is determined by treating it as a wheel of infinite radius, and its contribution is given by,

$$\phi_2 = \frac{p_o^2 a_o}{E_2} \left[ 0.9041 - 0.4292 v_2 + \left(\frac{a_o}{R}\right) \times \left\{ 0.1931 v_2 - 0.5235 + (0.5 - v_2) \ln\left(\frac{a_o}{R}\right) \right\} \right] \quad \dots \quad (26)$$

and neglecting  $(a_o/R)$  terms, it becomes

$$\phi_2 = \frac{p_o^2 a_o}{E_2} [0.9041 - 0.4292 v_2] \quad (27)$$

For energy losses in the flat surface, the co-efficient of rolling resistance is given by

$$\mu_2 = \frac{\phi_2}{N} \quad \dots \quad (28)$$

So, the overall co-efficient of resistance  $\mu$ , on substituting eqns. 25 and 23 in eqn. 7 is

$$\mu = \frac{1}{N} (\phi_1 + \phi_2) \quad \dots \quad (29)$$

Finally substituting for  $\phi_1$  and  $\phi_2$  from eqns. 24 and 27 respectively in eqn. 29 and substituting for  $p_0$  and  $\Delta$  from eqns. 8 and 9 respectively, yields

$$\mu = \frac{0.3247(1/E_1 + 1/E_2) - 0.1542(v_1/E_1 + v_2/E_2)}{\left[ \frac{1-v_1^2}{E_1} + \frac{1-v_2^2}{E_2} \right]^{1/2}} \quad (30)$$

$$\text{Now defining } \frac{1}{E} = \frac{1}{2} \left( \frac{1}{E_1} + \frac{1}{E_2} \right) \quad (31)$$

$$Q = N/ER \quad (32)$$

$$\text{and assuming } v_1 = v_2 = v \quad (33)$$

one gets,

$$\mu = \frac{0.4592 - 0.218 v}{(1-v^2)^{1/2}} (Q)^{1/2} \quad (34)$$

where  $E$  = equivalent Young's modulus and

$Q = N/ER$  = non-dimensional number named Chakra number.

As the Poisson's ratio of commonly used materials do not vary much, we can assume that the value of Poisson's ratio for the two dissimilar materials is same and is equal to 0.3.

So, by substituting  $v_1 = v_2 = v = 0.3$  in eqn. 34, we have for the plane stress case, co-efficient of rolling resistance

$$\mu = 0.4129145 (\alpha)^{1/2} \quad (35)$$

If  $(a_o/R)$  terms in the expressions for  $\phi_1$  and  $\phi_2$  are not neglected, and substituting the values of  $p_o$  and  $\Delta$  from eqns. 8 and 9 in eqns. 23 and 26 we have the values for  $\phi_1$  and  $\phi_2$  given by

$$\phi_1 = \frac{N^2}{E_1 a_o} \left[ 0.3142334 + \left( \frac{a_o}{R} \right) \cdot \left\{ \frac{0.8}{\pi^2} \ln \left( \frac{a_o}{R} \right) - 0.1907148 \right\} \right] \quad (36)$$

and

$$\phi_2 = \frac{N^2}{E_2 a_o} \left[ 0.3142334 + \left( \frac{a_o}{R} \right) \cdot \left\{ \frac{0.8}{\pi^2} \ln \left( \frac{a_o}{R} \right) - 0.1907148 \right\} \right] \quad (37)$$

For every load by calculating the 'half-contact-length',  $a_o$ , one can find out  $\phi_1$  and  $\phi_2$  and then substituting these values of  $\phi_1$  and  $\phi_2$  in the eqn. 29, one can determine the co-efficient of rolling resistance  $\mu$  if the radius of the wheel  $R$  and equivalent Young's modulus  $E$  are known.

(b) Plane strain case: Substituting the values of integrals  $I_1$ ,  $I_2$  and  $I_3$  in the expression for  $\phi_1$  of eqn. 19 yields,

$$\phi_1 = \frac{p_o^2 a_o}{E_1} \left[ (0.9041 - 0.4292 v_1 - 1.3333 v_1^2) + \left( \frac{a_o}{R} \right) \cdot \left\{ (0.1931 v_1 - 0.5285 + 0.7216 v_1^2) + (0.5 - v_1 - 1.5 v_1^2) \cdot \ln \left( \frac{a_o}{R} \right) \right\} \right] \quad (38)$$

As in the case of plane stress, eqn. 38 is further simplified by neglecting the terms containing  $(a_o/R)$  to

$$\phi_1 = \frac{p_o^2 a_o}{E_1} [ 0.9041 - 0.4292 v_1 - 1.3333 v_1^2 ] \quad (39)$$

Similarly, for energy losses in the flat surface, treating it as a wheel of infinite radius, the contribution is given by

$$\begin{aligned} \phi_2 = \frac{p_o^2 a_o}{E_2} [ & (0.9041 - 0.4292 v_2 - 1.3333 v_2^2) \\ & + \left(\frac{a_o}{R}\right) \cdot \left\{ (0.1931 v_2 - 0.5285 + 0.7216 v_2^2) \right. \\ & \left. + (0.5 - v_2 - 1.5 v_2^2) \cdot \ln \left(\frac{a_o}{R}\right) \right\} ] \quad (40) \end{aligned}$$

which can be further simplified to

$$\phi_2 = \frac{p_o^2 a_o}{E_2} [ 0.9041 - 0.4292 v_2 - 1.3333 v_2^2 ] \quad (41)$$

by neglecting  $(a_o/R)$  terms.

Finally, substituting for  $\phi_1$  and  $\phi_2$  from eqns. 39 and 41 respectively in eqn. 29 and substituting for  $p_o$  and  $\Delta$  from eqns. 8 and 9 respectively, yields the co-efficient of rolling resistance  $\mu$  as

$$\mu = \frac{0.3247 \left( \frac{1}{E_1} + \frac{1}{E_2} \right) - 0.1542 \left( \frac{v_1}{E_1} + \frac{v_2}{E_2} \right) - 0.4789 \left( \frac{v_1^2}{E_1} + \frac{v_2^2}{E_2} \right)}{\left[ \frac{1-v_1^2}{E_1} + \frac{1-v_2^2}{E_2} \right]^{1/2}} \cdot \left( \frac{N}{R} \right)^{1/2} \quad (42)$$

By using eqns. 31, 32 and 33, eqn. 42 can be rewritten as,

$$\mu = \left[ \frac{0.4592 - 0.218 v - 0.6772 v^2}{(1-v^2)^{1/2}} \right] (\Omega)^{1/2} \quad (43)$$

where,  $\Omega = \frac{N}{E_R} = \text{Chakra number.}$

By taking the numerical value of Poisson's ratio  $v = 0.3$ , we have

$$\mu = 0.3489236 (\Omega)^{1/2} \quad (44)$$

If the terms containing  $(a_o/R)$  are not neglected in the expression for  $\phi_1$  and  $\phi_2$ , and substituting the values of  $p_o$  and  $\Delta$  from eqns. 8 and 9 in eqns. 38 and 40, we have the values of  $\phi_1$  and  $\phi_2$  respectively

$$\phi_1 = \frac{N^2}{E_1 a_o} \left[ 0.2656005 - \left( \frac{a_o}{R} \right) \cdot \left\{ 0.164394 - 0.026 \ln \left( \frac{a_o}{R} \right) \right\} \right] \quad (45)$$

and

$$\phi_2 = \frac{N^2}{E_2 a_o} \left[ 0.2656005 - \left( \frac{a_o}{R} \right) \cdot \left\{ 0.164394 - 0.026 \ln \left( \frac{a_o}{R} \right) \right\} \right] \quad (46)$$

Substituting the values of  $\phi_1$  and  $\phi_2$  in eqn. 29 one can obtain the value of co-efficient of rolling resistance,  $\mu$ .

Thus, we have, analytically, four different expressions for  $\mu$ , one accurate and one simplified expression in each of the plane stress and plane strain cases. Equations 35 and 44 gives simplified expressions for  $\mu$  in plane stress and plane strain cases respectively, where as, resulting expressions obtained by substituting eqns. 36 and 37 and eqns. 45 and 46 in eqn. 29 gives accurate



expressions for  $\mu$  in plane stress and plane strain cases respectively.

Theoretical curves are plotted in Fig. 3 on ordinary graph and Fig. 4 on semi-log graph showing  $\mu$  vs  $Q$ , in plane stress and plane strain conditions. Fig. 3 shows a parabola, indicating the square-root dependence of  $\mu$  on  $Q$ . On calculations, one can find the difference between the simplified and accurate expression is within 4% for a  $Q$  value as high as 250 which corresponds to  $\mu_{\text{plane stress}}=0.0065$  and  $\mu_{\text{plane strain}}=0.0055$ . For lower values of  $Q$ , this difference is within 1% and hence we can use only simplified expressions in both cases of plane stress and plane strain. In plotting the Figs. 3 and 4 only these simplified expression are used. The theoretical curves show that the values of  $\mu$  in plane stress condition are 15.48% higher than that of plane strain condition. In actual situation, as we donot know whether it is plane stress or plane strain, it is expected that the experimental values may lie between these values.

Eqns. 35 and 44 clearly establish that the coefficient of rolling resistance is directly proportional to the square-root of the dimensionless group  $Q = \frac{N}{ER}$ . The relation between  $\mu$ , and equivalent Young's modulus ( $E$ ), is of inverse square-root and therefore, a body with a lower equivalent Young's modulus causes more energy losses.

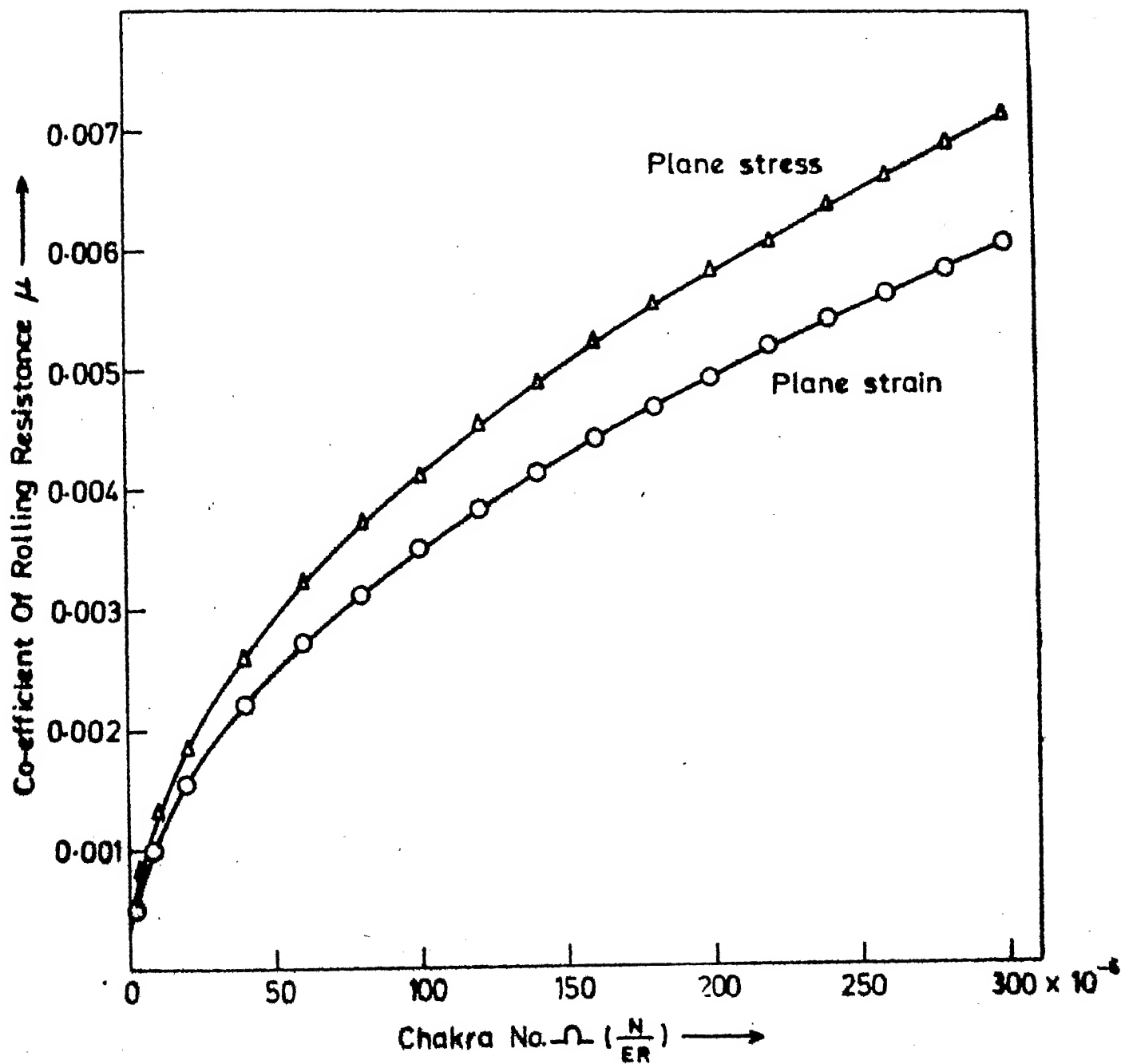
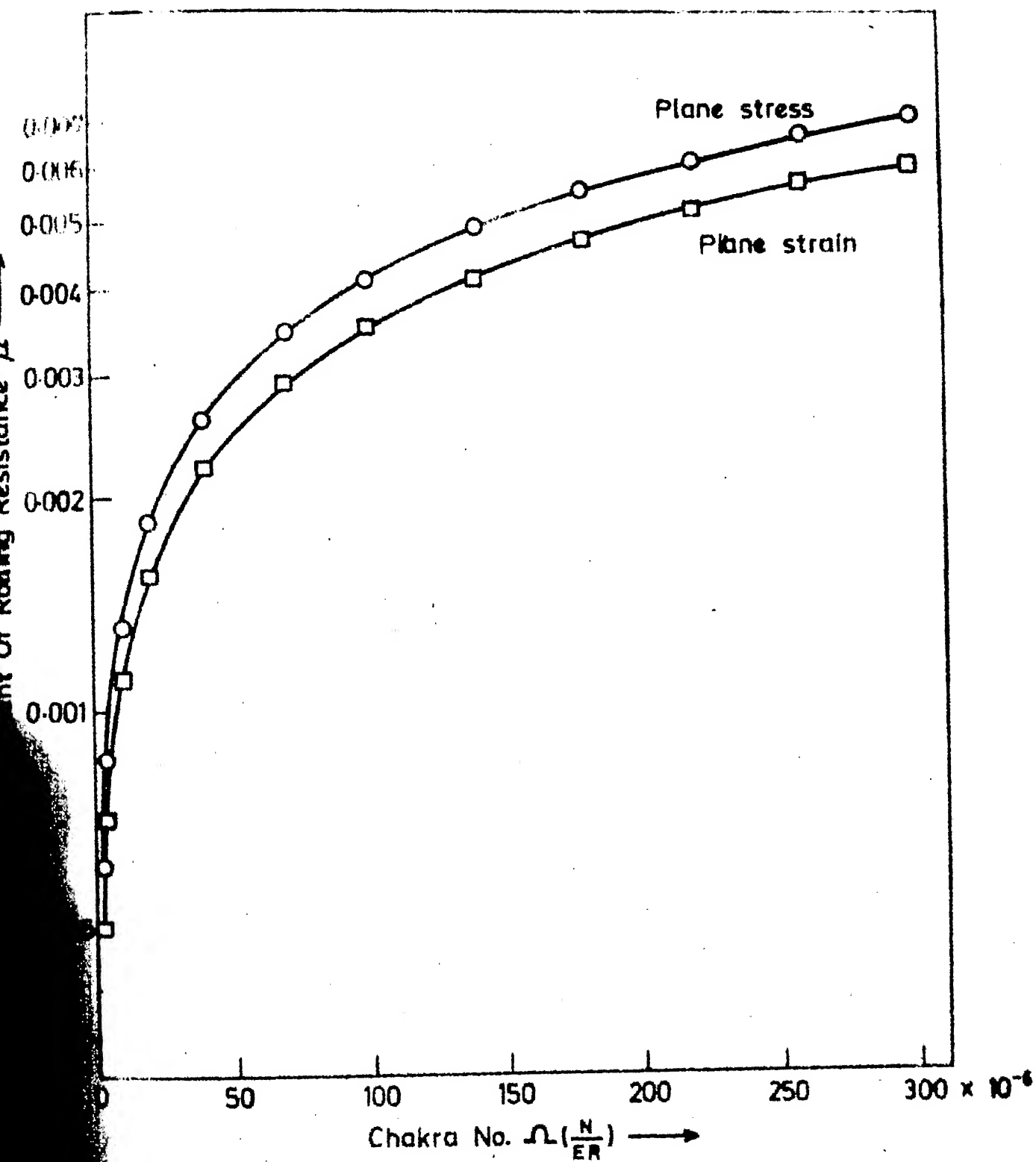


Fig. 3 Theoretical curves for  $\mu$  vs  $\Omega$  under plane stress and plane strain conditions.



Theoretical curves for  $\mu$  vs  $\Omega$ .

Whether a hard wheel of steel rolls on a relatively soft plastic surface, or a plastic wheel rolls on a hard steel surface - doesnot make much of a difference as far as energy losses are concerned. In case of a hard wheel rolling on a soft surface, the latter stores more strain energy. Similarly for a soft wheel rolling on a hard surface, the major effect of energy losses is due to larger deformation of wheel.

The co-efficient of rolling resistance is directly proportional to the square root of the applied load per unit width of the wheel. The result is valid for all ranges of load as long as they donot cause yielding in the materials. Experimental results are not available for the rolling of an elastic wheel of uniform width on an elastic surface. However Drutowski [8] conducted experiments by rolling 12.7 mm diameter steel balls on steel plate. The co-efficient of rolling resistance, even in the elastic range was observed to be dependent on  $N$ . It was found to be proportional to  $N^{0.2}$ . This result of spherical balls can not be compared quantitatively with the analytical results of  $\mu \propto N^{0.5}$ , of wheels, because of the difference in the shapes of the rolling bodies. Nevertheless one concludes that co-efficient of rolling resistance increases with increasing load.

Furthermore, the co-efficient of rolling resistance is inversely proportional to the square-root of the radius of the wheel. In case of a small wheel, contact stresses for a given load are high as the contact area is small. The high stresses develop large strain energy in the rolling bodies which in turn causes high energy losses. In the case of a spherical ball rolling elastically on a flat surface,  $\mu$  has been experimentally measured by Bowden and Tabor [2]. It was found to be proportional to  $1/R^m$ , where the exponent  $m$  lies between 1.5 and 1.6. The large values of the exponent  $m$  is because of much smaller area of contact of rolling balls in comparison to that of wheels. Hence the losses due to increase in strain energy density become higher. Even in the case of pneumatic tyres rolling on concrete surface,  $\mu$  is observed [12] to be proportional to  $1/R^m$ , where  $m$  is close to unity. Thus, the co-efficient of rolling resistance is proportional to  $1/R^m$  where  $m$  depends on the shapes of the rolling surfaces.

## CHAPTER-IV

### EXPERIMENTAL ARRANGEMENT

Scientifically reported results of energy losses of a wheel rolling over a flat surface are not available in literature, and therefore, an experimental set-up is devised to determine the co-efficient of rolling resistance under controlled conditions. The rolling surfaces are chosen to be smooth to minimize undesirable jumping of the wheel, and from this consideration, a disc shaped wheels of plexi-glass and teflon are selected to roll over a flat and horizontally are levelled surface of plexi-glass. The effect is further reduced by rolling the wheel at a very low speed within the range of 0.06 to 0.15 m/sec at which losses due to impact mechanism of wheel on the flat surface are negligible.

The wheel is given an initial velocity through a guide ramp located on one side of the flat surface as shown in Fig. 5, the schematic diagram of the experimental arrangement. Instead of using two separate strips of plexi-glass for flat surface and ramp, one single long strip has been used so that the vibrations that develop

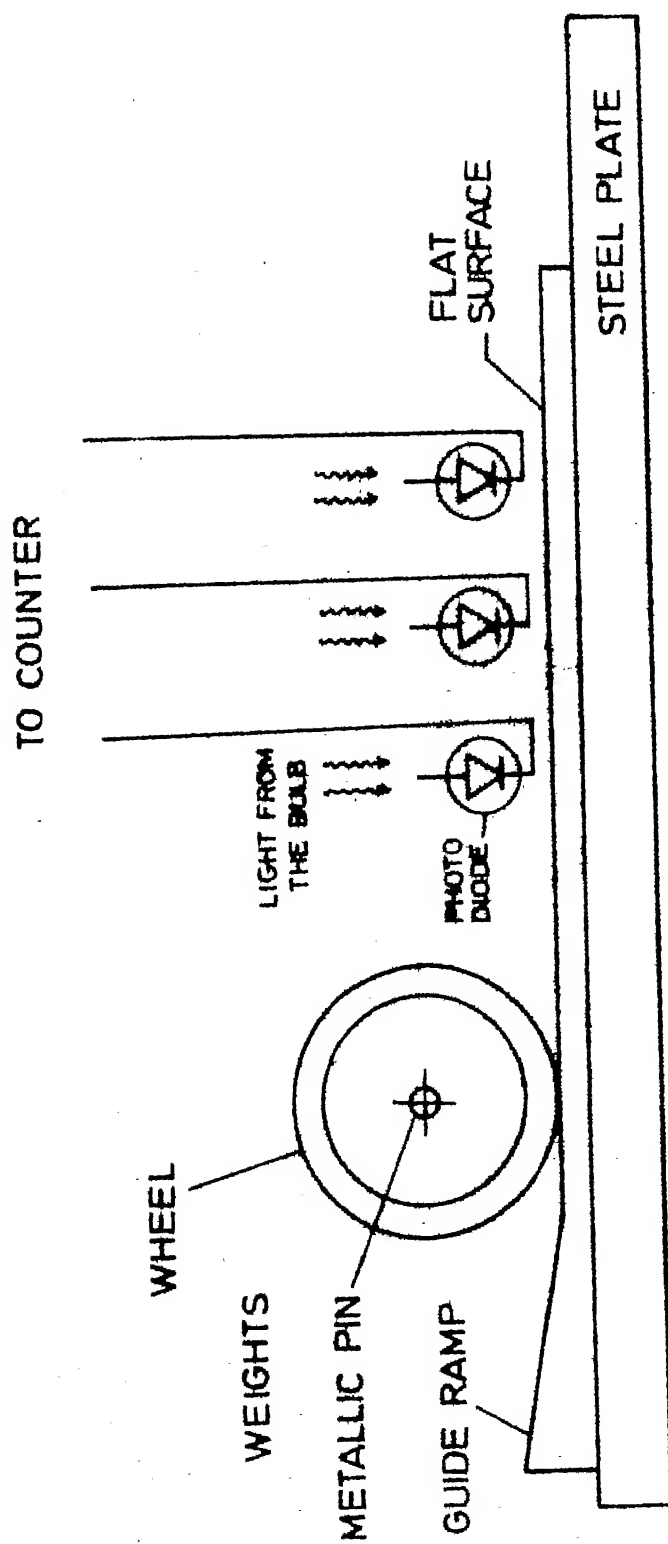


Fig. 5 Schematic diagram of the experimental arrangement.

due to the joint between the ramp and flat surface have been minimized. Fig. 6 shows the overall view of the arrangement and Fig. 7 shows a close view of the plexi-glass wheel, attached with aluminium disc weights.

In the experiment, the wheel is mounted centrally over a 135 mm long externally threaded mild steel tube, fastened on two ends by circular brass nuts. The surfaces of the wheels are prepared smooth with fine sand papers and buffing. Load on the wheel is varied by changing the attached disc weights. There are as many as seven wheels on which experiments are conducted, of which two are made of Teflon and five are made of plexi-glass. The materials are chosen to have a large difference in their Young's moduli. Young's modulus for Teflon is 300 MPa and that of plexi-glass is 2307.7 MPa. These values are obtained by conducting compression tests on two specimens of plexi-glass and seven specimens of Teflon on an Universal Testing Machine, INSTRON 10. Typical compression curves are shown in Figs. 8 and 9 respectively for plexi-glass and Teflon.

Some of the wheels were square-grooved in the centre of the rolling surface as in Fig. 10 so that the value of  $N$  (load per unit thickness) is varied for the same weight attached. Further, wheels of different diameters have been used. Table No. 1 gives the



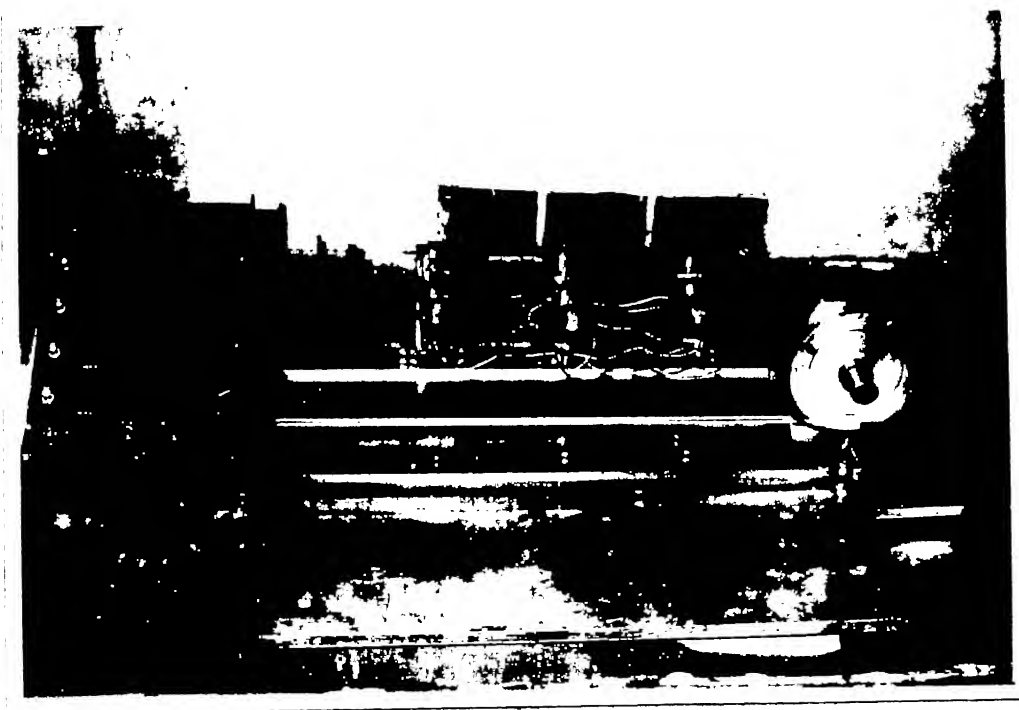


FIG. 6 : OVERALL VIEW OF WHEEL ROLLING EXPERIMENTAL SET-UP.

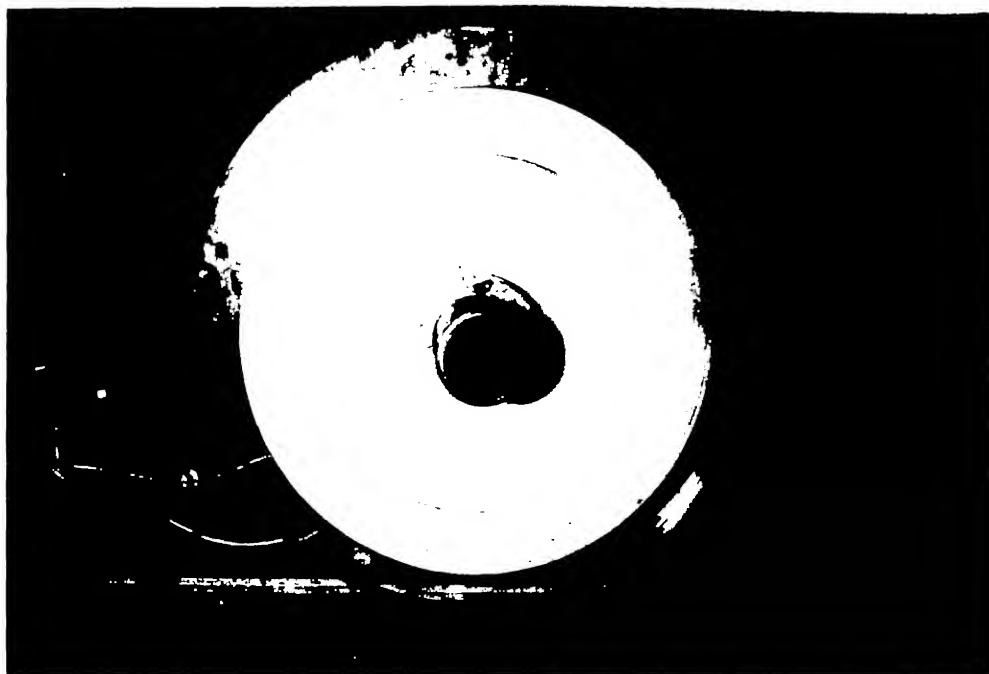


FIG. 7 : CLOSE-VIEW OF THE PLEXI-GLASS WHEEL  
ATTACHED WITH DISK SHAPED ALUMINIUM  
WEIGHTS.

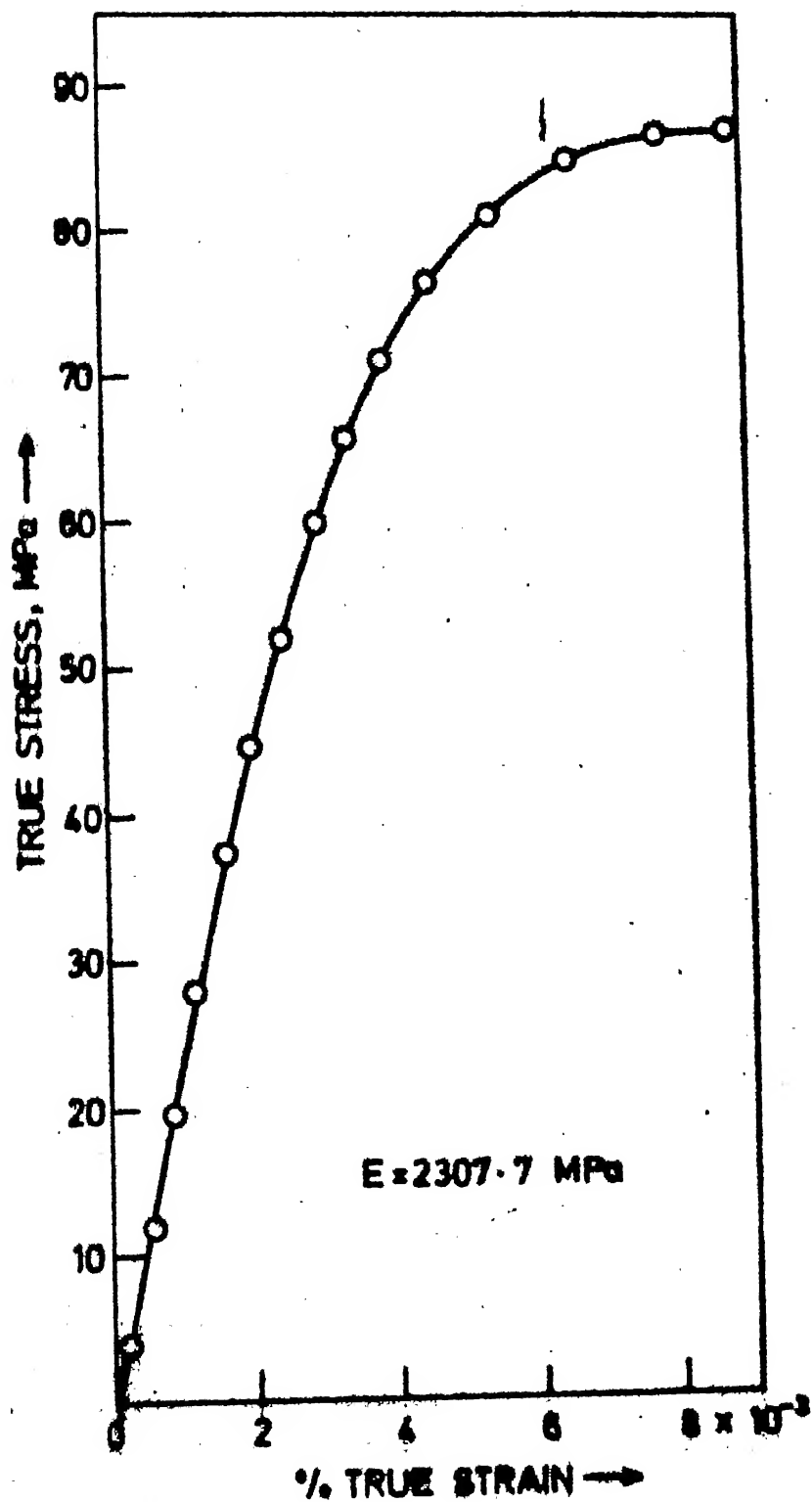


Fig.8 Stress-Strain curve for Plexi-glass material under compression.

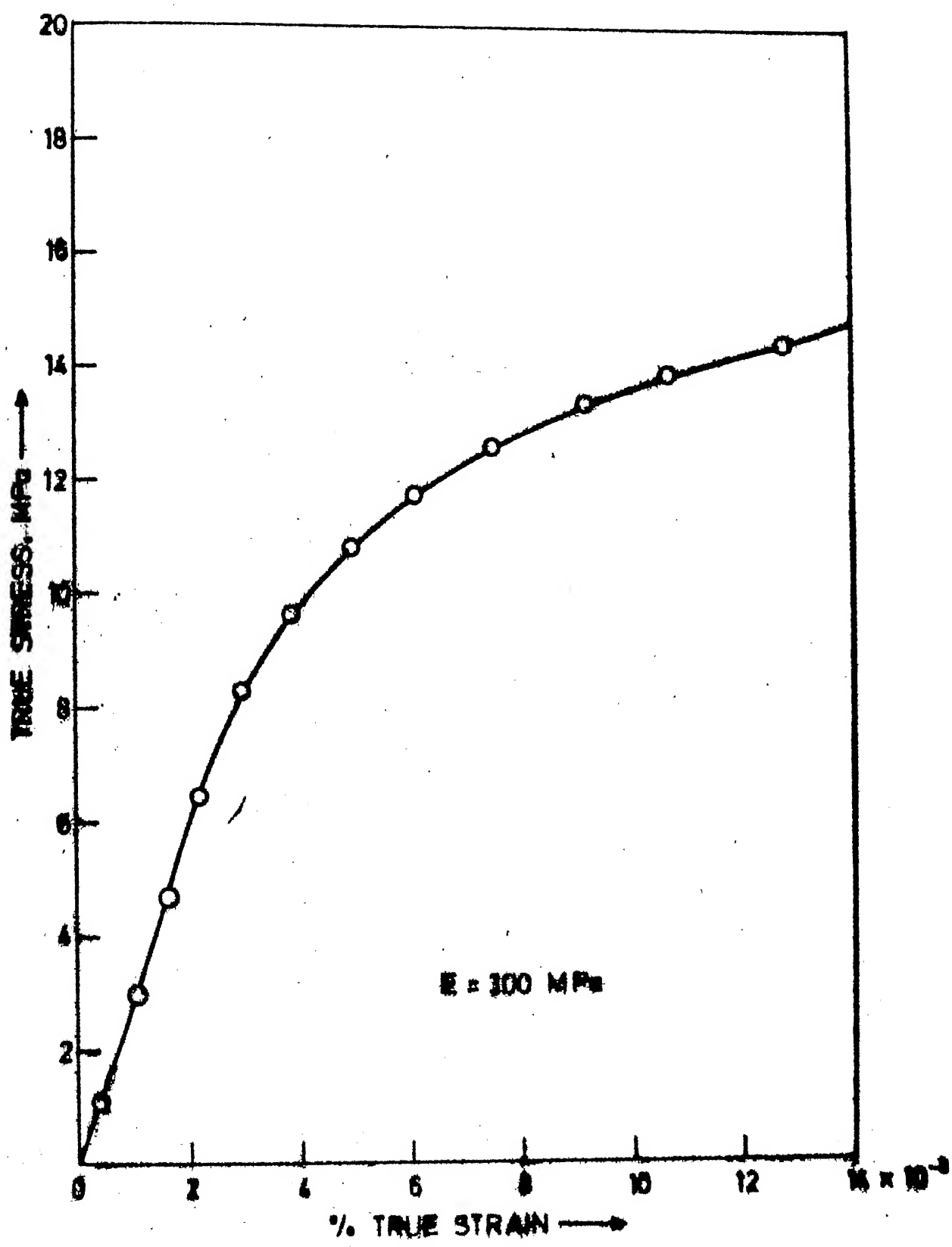


Fig. 2. Stress-strain curve for Teflon material under compression.

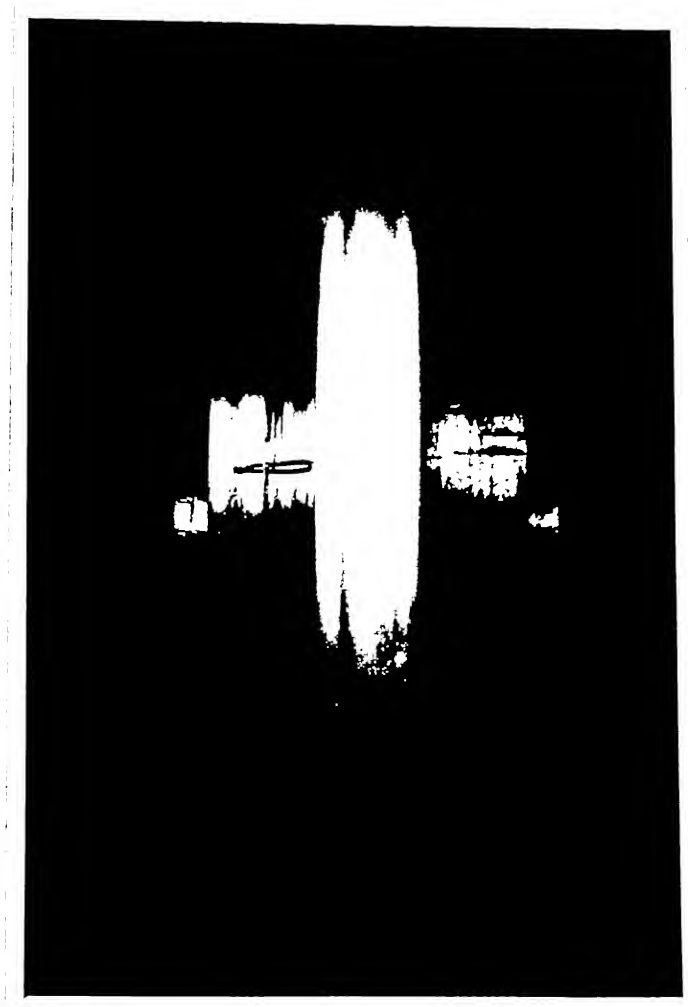


FIG. 10 : CLOSE VIEW OF THE ROLLING SURFACE  
OF GROOVED TEFLON WHEEL.

(i) widths of contact surfaces, (ii) radii, (iii) Young's Moduli, (iv) loads and (v) materials - of the different wheels. Thus by using this set-up one can verify the relation between the co-efficient of rolling resistance  $\mu$  and all the above parameters  $N$ ,  $E$  and  $R$  or the 'Chakra No.'

$$Q = \frac{N}{ER} .$$

The flat surface is a 10 mm thick, 750 mm long strip, with the breadth equal to 90 mm. One end of the strip is reduced to fit into the guide ramp. The strip is chosen from commercially available plexi-glass sheets and is placed on the top of a rigid 25 mm thick, 630 mm square aluminium surface plate, and bolted at the two ends. Aluminium surface plate, supported over three specially designed levelling screws, is placed over a suitable masonry foundation. The guide ramp is also mounted on three levelling screws so that one can change the slope of the ramp there by change the velocity of the wheel.

The wheel is given an initial velocity through the guide ramp located on one end of the flat surface as in Fig. 6. Due to energy loss in the rolling process, the velocity of the wheel gradually reduces. During its rolling over the flat surface, the wheel passes through three stations  $F_1$ ,  $F_2$ , and  $F_3$ . Each of the three stations consists of a 145 mm high vertical stand with a tripodal base screwed over a base strip. Each stand is

'F' shaped with top cantilever is fitted with a 28 V bulb and lower cantilever is fitted with a photo-diode, almost fully covered except a small hole of 3 mm diameter. So, if the bulb emits light, it will have to pass through the small, 3 mm dia. aperture to reach the photo-diode. Then photo-diode will send the signal to the counter, which counts the time. The digital time interval counter used is custom made, 4 channel timer, with the accuracy of  $1 \mu \text{ sec}$  by Networks Co., KANPUR. Close view of photo-diode arrangement is shown in Fig. 11. Photodiode circuit diagrams and components used in it are shown in Fig. 12. During rolling, a 15 mm long brass pin of 2 mm. diameter fixed at the axis of the wheel, passes between the two cantilevers of each of the stations  $F_1$ ,  $F_2$  and  $F_3$ , so that it can obstruct the path of light at each station. As it obstructs the path of light of  $F_1$  from the bulb to the photo-diode, momentarily, voltage signal from the photo-diode to the counter will be stopped. The circuit was designed to start counting the time in micro-seconds from that moment onwards in the first channel of the timer counter. As soon as the wheel reaches station  $F_2$ , again the pin obstructs the path of light from second bulb to second photo-diode, hence voltage signal from the second photo-diode to the counter stops momentarily. The circuit is designed to stop counting the time in the first channel of

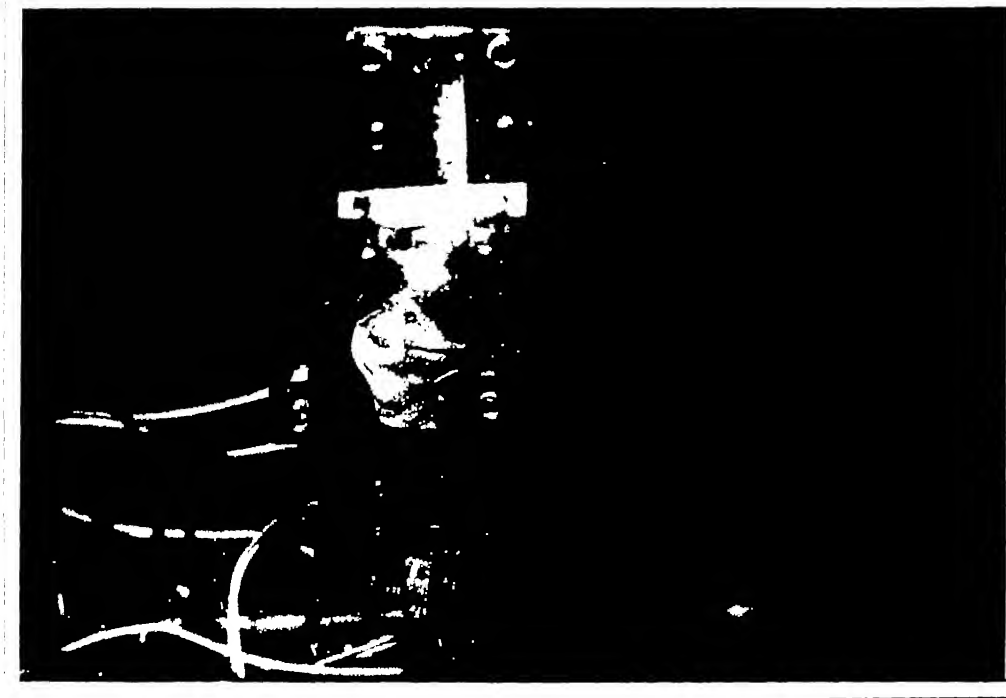


FIG. 11 : CLOSE VIEW OF THE PHOTO-DIODE  
ARRANGEMENT.



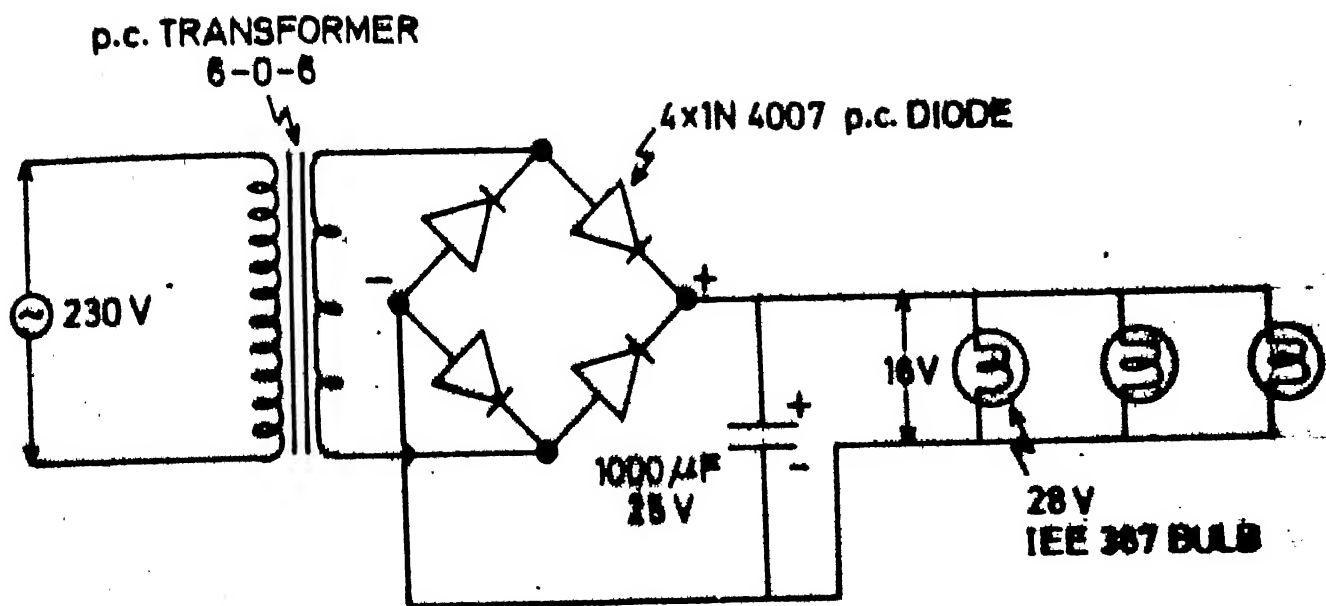


Fig.12 a Circuit diagram for bulbs.

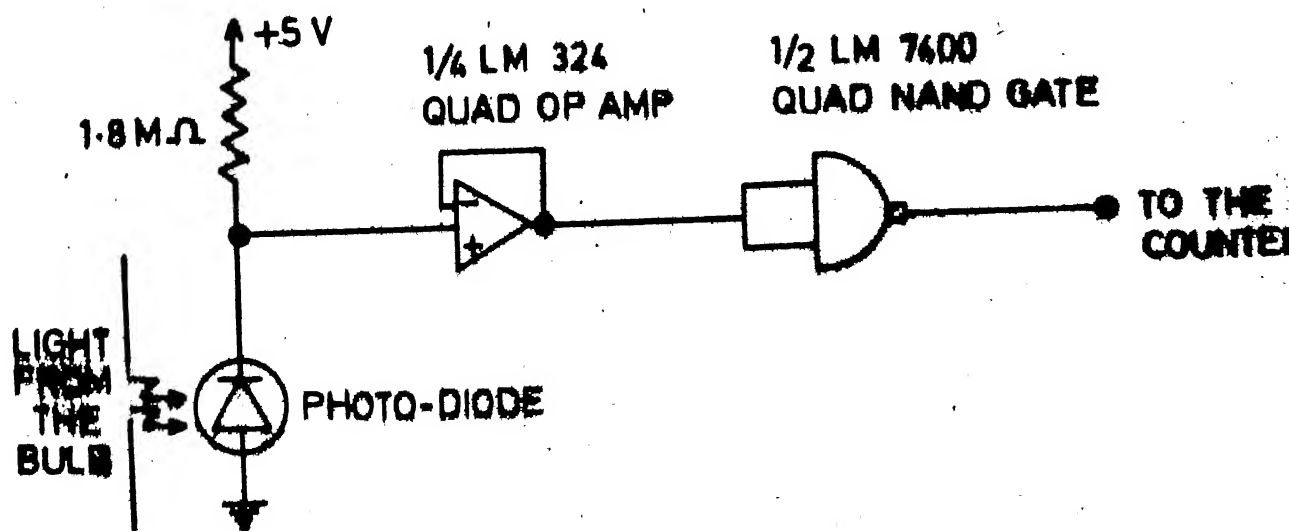


Fig.12 b Circuit diagram for a photo-diode.

the timer counter and to start counting the time in the second channel of the timer counter from this moment onwards. As the wheel reaches  $F_3$ , again the brass pin obstructs the path of light and counting of time in the second channel of the timer counter stops immediately. Thus from the timer counter we can read the exact value of time taken by the wheel to reach  $F_2$  from  $F_1$  and  $F_3$  from  $F_2$  with the accuracy of  $1 \mu \text{ sec}$ . These time intervals can be named  $t_1$  and  $t_2$  respectively. The distances between the stations are named as  $l_1$  and  $l_2$  respectively from  $F_1$  to  $F_2$  and from  $F_2$  to  $F_3$ . The distances  $l_1$  and  $l_2$  are measured accurately within 0.5 mm.

Since the tests were conducted on wheels of different diameters, arrangement is made for fixing the two cantilevers, to the stand, at any required height. That is, one can keep the photo-diode and bulb arrangement at the required height depending on the height of the wheel so that the brass pin at the axis of the wheel comes in between the bulb and the photo-diode to obstruct the path of light.

The acceleration of the wheel is expressed in terms of an equivalent pulling force  $F$ . Since the pulling required to overcome the rolling resistance ( $F = \mu N$ ) is constant for a given load, acceleration is assumed to be constant and easily expressed in terms of experimentally measured quantities by the equation

$$a = \frac{2 (l_2 t_1 - l_1 t_2)}{t_1 t_2 (t_1 + t_2)} \quad (47)$$

The change in the kinetic energy  $\Delta K$  of a freely rolling wheel is equal to the equivalent work done, and therefore,

$$\Delta K = F \cdot dS \quad (48)$$

Also,  $\Delta K$  for a rolling wheel can be expressed in terms of linear acceleration,  $a$ , and the angular acceleration  $\alpha$ , by the equation,

$$\Delta K = m a dS + m k^2 \alpha d\theta \quad (49)$$

where,  $m$  is the mass,  $k$  is the radius of gyration of the wheel and  $\theta$  is the angular rotation. Substituting eqn. 48 in eqn. 49 for  $\Delta K$  and using the relations  $\alpha = a/R$  and  $d\theta = \frac{dS}{R}$ , one gets

$$F = m a \left(1 + \frac{k^2}{R^2}\right) \quad (50)$$

And, by substituting the value of  $F$  from eqn. 4 and noting that  $N = m g$ , one can obtain the co-efficient of rolling resistance

$$\mu = \frac{a}{g} \left(1 + \frac{k^2}{R^2}\right) \quad (51)$$

where,  $g$  is the acceleration due to gravity. However, the slope of the flat surface, if any, will cause a component of the acceleration due to gravity to act along

the plane of the flat surface in addition to the acceleration,  $a$ . If  $\beta$  is the slope of the flat surface with respect to the horizontal plane, net acceleration comes to

$$a = \left[ \frac{\mu}{\left(1 + \frac{k^2}{R^2}\right)} + \sin \beta \right] \cdot g$$

In order to minimize the effect of gravitation, the flat rolling surface as mentioned earlier, is mounted on three levelling screws and a spirit-level with a least count of 0.1 m. rad is used. Furthermore, a relatively soft plexi-glass (polymethyl methacrylate) and Teflon are chosen as materials for wheel and plexi-glass is chosen as material for flat surface so that the term  $\frac{\mu}{\left(1 + \frac{k^2}{R^2}\right)}$  in eqn.

52 dominates. For an expected value of  $\mu = 0.002$ , the maximum permissible slope of the flat surface is 0.13 m. rad, if the contribution of gravitational forces is limited to 10% of rolling acceleration.

## CHAPTER-V

### RESULTS AND DISCUSSIONS

Experiments are conducted for twenty eight values of load per unit width,  $N$ , using five plexi-glass wheels and two Teflon wheels of different diameters and thicknesses as given in Table No. 1. The wheels are rolled on a 90 mm wide and 10 mm thick plate of plexi-glass. On each wheel, two to five values of  $N$  are obtained by varying the disc shaped weights made of aluminium and cast iron attached to the wheel. The weights are used in pairs on either side of the wheel so that mechanical imbalance is minimum during rolling. Also rolling speeds are kept within a low range of 0.06 to 0.15 m/sec and in each case the wheel is rolled about 40 times.

#### (A) Plexi-glass Wheels Rolling on a Plexi-glass Flat Surface:

The experimental values of co-efficient of rolling resistance,  $\mu$ , together with theoretical values for plane stress and plane strain and Chakra Number  $Q$  ( $N/ER$ ) are tabulated in Table No. 2. Taking these values,  $\mu$  vs  $Q$  curves are plotted in Figs. 13 and 14 for ordinary and semi-log scales respectively.

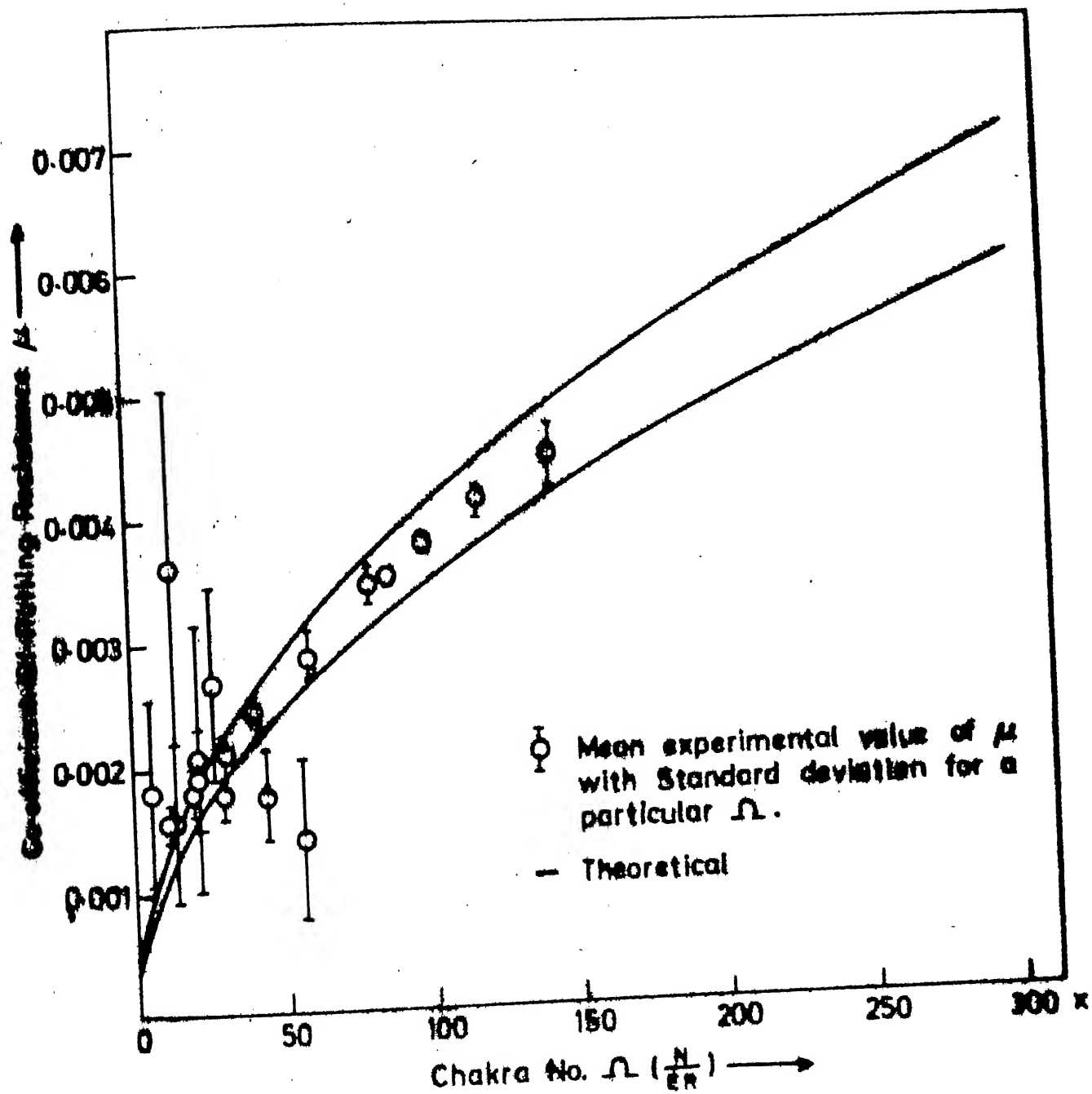
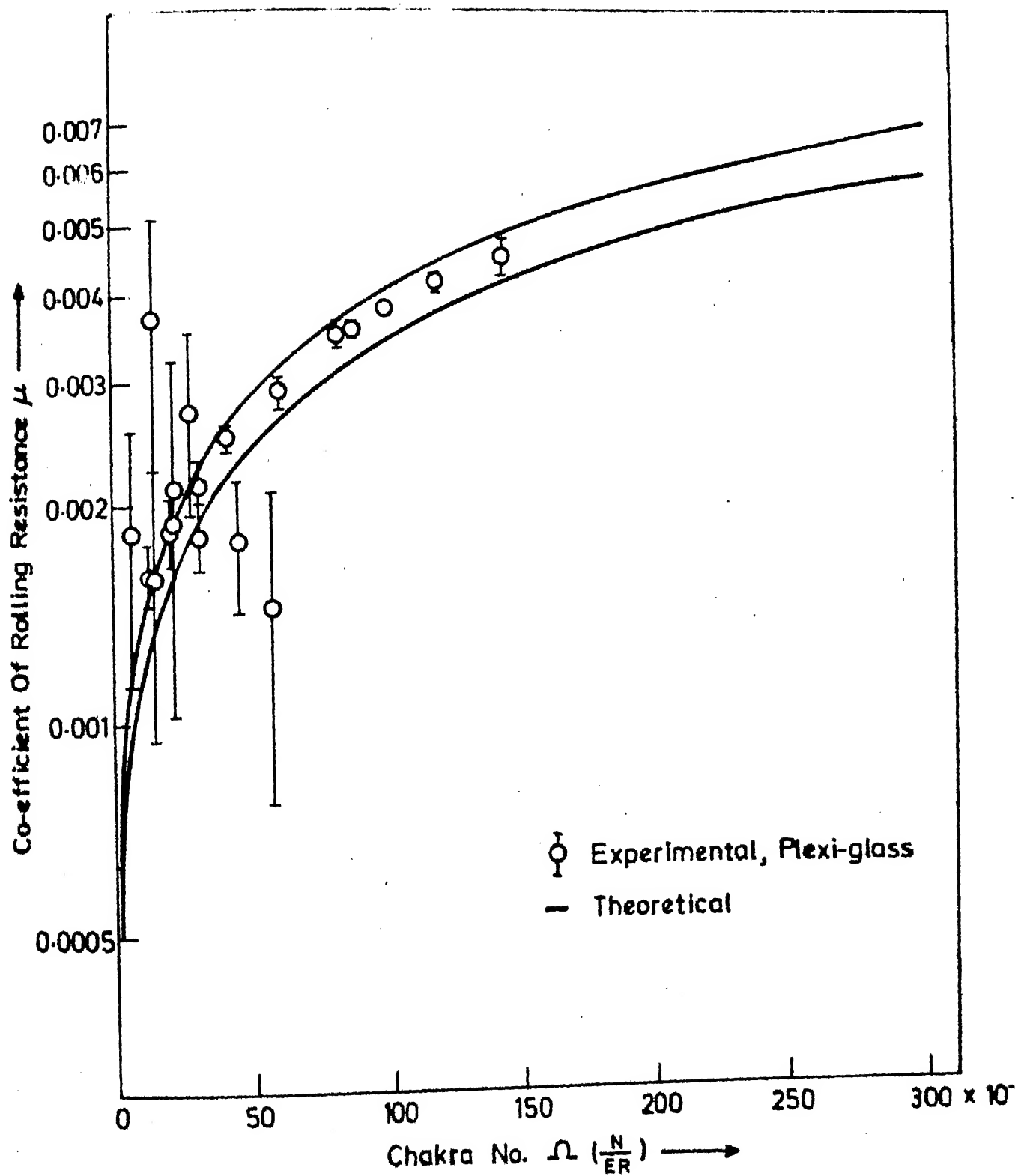


Fig.13  $\mu$  vs  $\Omega$  for Flexi-glass wheels on Flexi-glass flat surface.



— Plexi-glass flat surface.

From these graphs, we observe that the average values of  $\mu$  increases with Chakra No.  $Q$ . Also in 11 sets out of 20 sets of readings, the average value of  $\mu$  lies in between the two theoretical curves of plane stress and plane strain. At low loads, experimental parameters are difficult to control as vibrations and other effects such as local imperfections in flatness come into picture. Hence, the average values of  $\mu$  are rather scattered at low  $Q$ .

The values of  $\mu$  are more close to plane stress, specially for high values of  $Q$ , where the webs of the wheel are thin because a groove on the rolling surface was machined out centrally to increase load per unit thickness ( $N$ ). These webs are about 2.25 mm thick as against 19 mm thick wheel of lower  $Q$  values. Consequently the webs are loaded mainly in plane stress.

Hasnain [10] conducted the experiment only for three values of  $Q$  using a 19 mm thick plexi-glass wheel on a plexi-glass flat surface. His results along with the results of present study are shown in Fig. 15. While Hasnain conducted his experiments by varying  $Q$  between 6 and 26.5, the range of  $Q$  in the present study has been increased to  $Q = 142$ . Results for all the three points of Hasnain's work lie very close to theoretical prediction for rolling

CENTRAL LIBRARY  
Kanpur.

Acc. No. A 82409



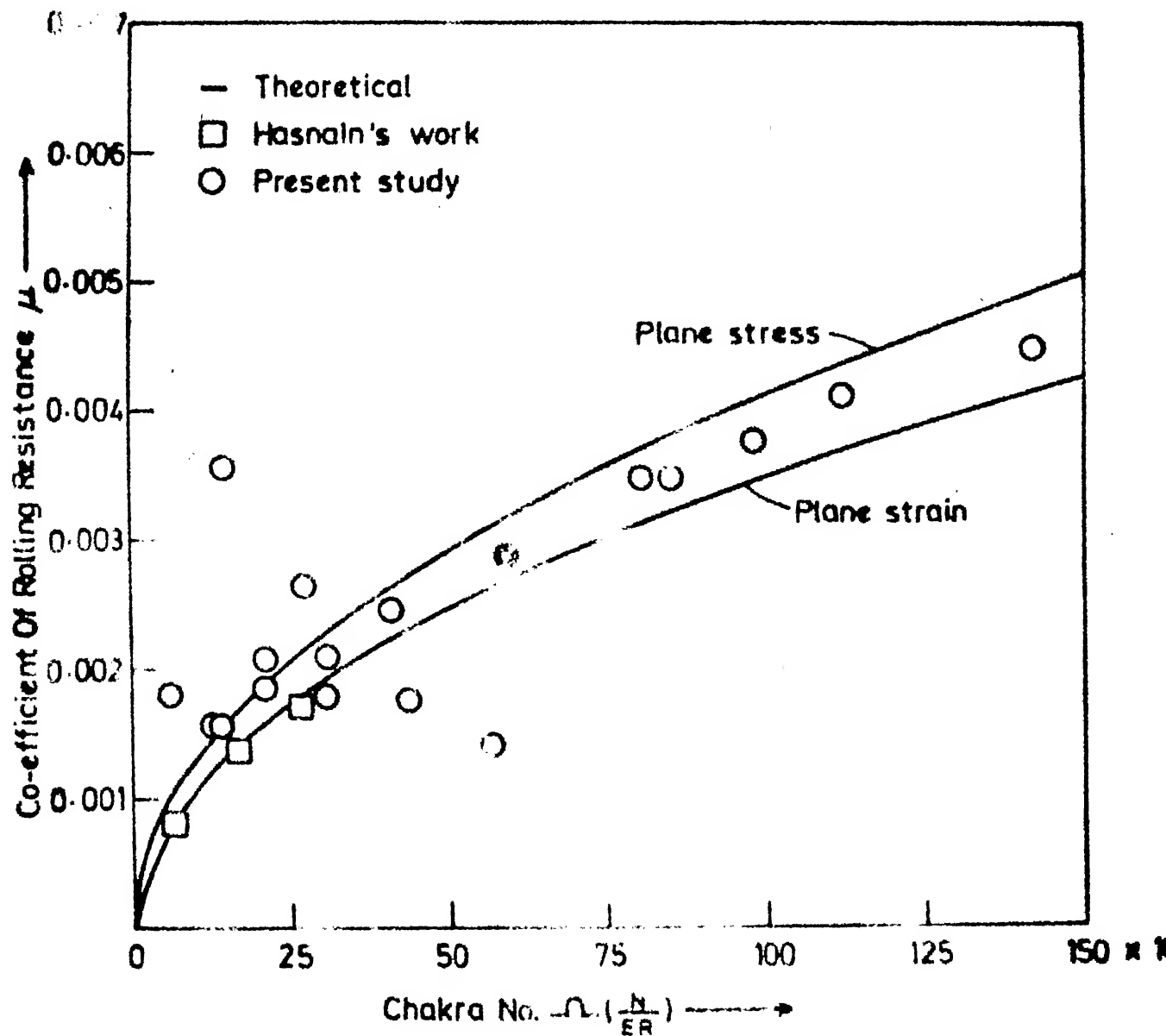


Fig.15 Comparison of Hasnain's results with the present study.

in plane strain mode. This is understandable, as the wheel was thick and the loading was closer to plane strain. In the present study, most of the experiments conducted with thin webbed wheels and the results lie between plane stress and plane strain curves. However, the scatter at low Chakra Number  $Q$  (upto 57) was large and the reasons are not understood well.

The Chakra Number was further extended to 263 by employing a low modulus wheel of Teflon as described in the next section.

(B) Teflon Wheels on Plexi-glass Flat Surface:

Teflon is chosen to increase  $Q = \frac{N}{ER}$ . Hasnain could not vary the  $Q$  by large amounts and in his experiment maximum value of  $Q$  is 26.5. Chakra No.  $Q$  can be increased either by increasing  $N$  or by reducing  $E$  or  $R$  or both. Increasing the  $N$  (load per unit thickness of wheel) can be achieved either by increasing the loads on the sides of the wheel or by decreasing the thickness of webs on each side of the groove. The diameter of the side weight is limited by the diameter of the wheel and too thick side weights cause vibrations during rolling. The webs can not be made very thin, as the load may reach a point where the state of stress induced in the wheel is such that, stress-strain relations may not be linear are no longer linear. Another

alternative might be to decrease the radius of a wheel  $R$ . But due to experimental limitations,  $R$  could not be decreased much. If  $R$  is reduced, thickness of the side weights increases substantially to maintain the same load per unit thickness  $N$  of a wheel and then side weights with large thicknesses cause vibrations. Also diameter of the side weight is limited by the diameter of the wheel. Hence reduction in  $R$  is not helpful in increasing  $Q = \frac{N}{ER}$ .

As in the case of plexi-glass wheels, grooves are provided in the wheel so that effective thickness decreases and load per unit thickness,  $N$ , increases. To reduce  $E$ , a low modulus material, Teflon is chosen as a wheel material whose Young's modulus is 8 times less than that of plexi-glass.

The experimental values of  $\mu$  together with theoretical values and Chakra No.  $Q$  are tabulated in Table No. 2. For these values,  $\mu$  vs  $Q$  curves are plotted in Figs. 16 and 17 on ordinary and semi-log scale respectively.

From these graphs, we can conclude that the average value of  $\mu$  increases with Chakra No.  $Q$ , as in the case of plexi-glass wheel rolling on a plexi-glass surface. However, all the values obtained experimentally are less than theoretically predicted plane strain values. Hence,  $\mu$  for this case is slightly different from the plexi-glass

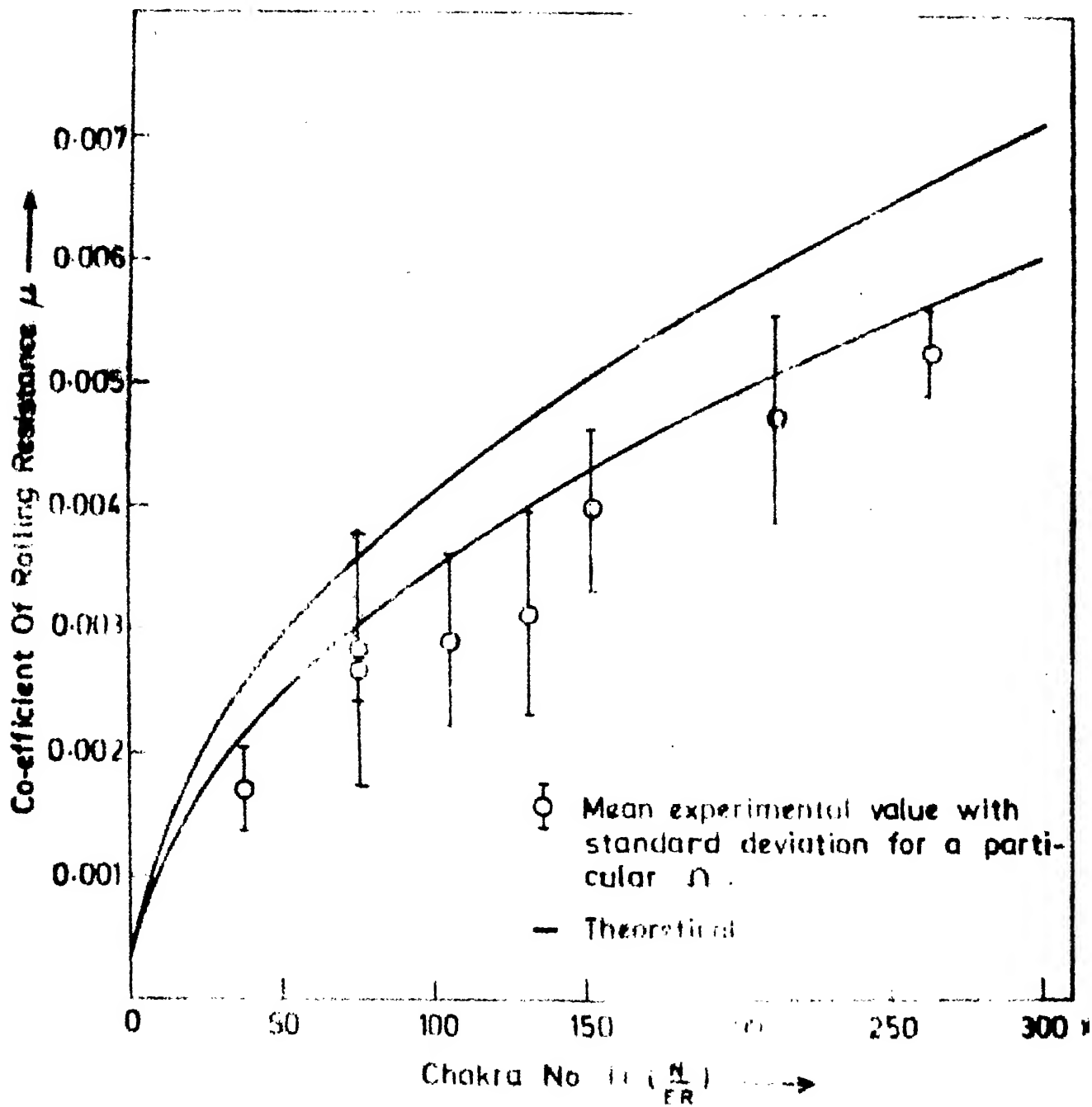


Fig.16  $\mu$  vs  $\Omega$  for teflon wheels on Plexi-glass flat surface

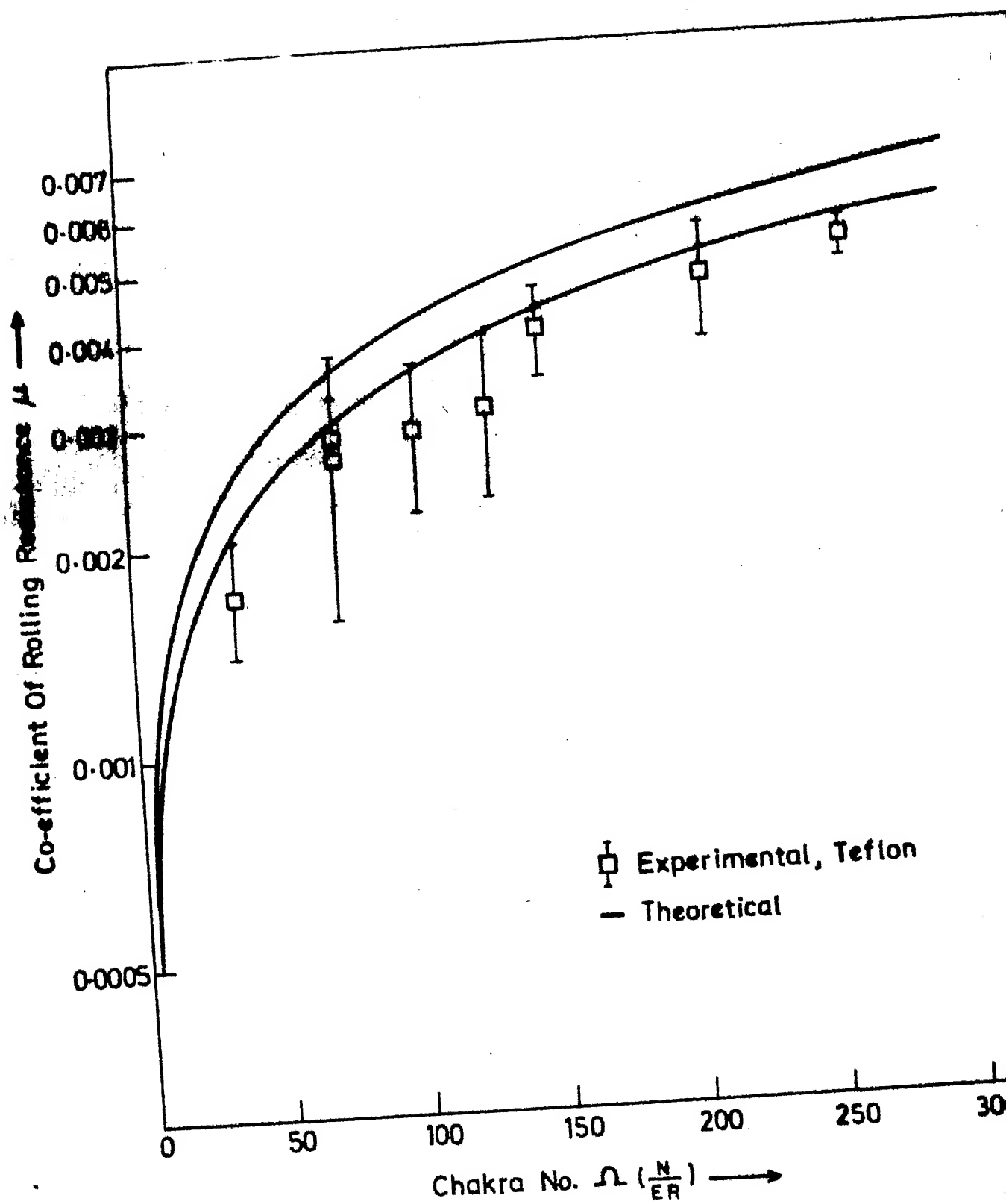


Fig.17  $\mu$  vs  $\Omega$  for Teflon wheels on Plexi-glass flat surface.

wheel rolling on plexi-glass surface. Hence Teflon wheels are loaded more in plane strain than in plane stress. However the fact that  $\mu$  lies outside the zone between plane stress and plane-strain, but very close to plane strain curve can be due to other factors such as sliding or other experimental limitations, or due to not using the correct value of Poisson's ratio. It may also be due to the fact that the entire strain energy which is in the sector at the bottom of the wheel is not released but a part of it is utilized in rolling the wheel further. This need to be probed further.

Typical data for two sets of observations together with calculations are tabulated in Table No. 4(a) and (b). This table lists the average value of  $\mu$  with standard deviation.

The overall graphs, for all the twenty eight values of  $N$  and experimentally obtained values of  $\mu$  together with theoretical curves are shown in Figs. 18 and 19 respectively on ordinary and semi-log scales.

From these Figs. one can conclude that for large values of  $Q$ ,  $\mu$  is close to predicted value. Also corresponding to a value of  $Q = 250$ ,  $\mu = 0.6\%$  which is, on the high-side of the most of the devices used under rolling friction such as in rail-roads, rolling bearings etc. In fact, it hardly goes beyond  $0.3\%$ . So experiments upto a value of  $Q = 250$  are sufficient to test the practical validity of the theoretical formulation.

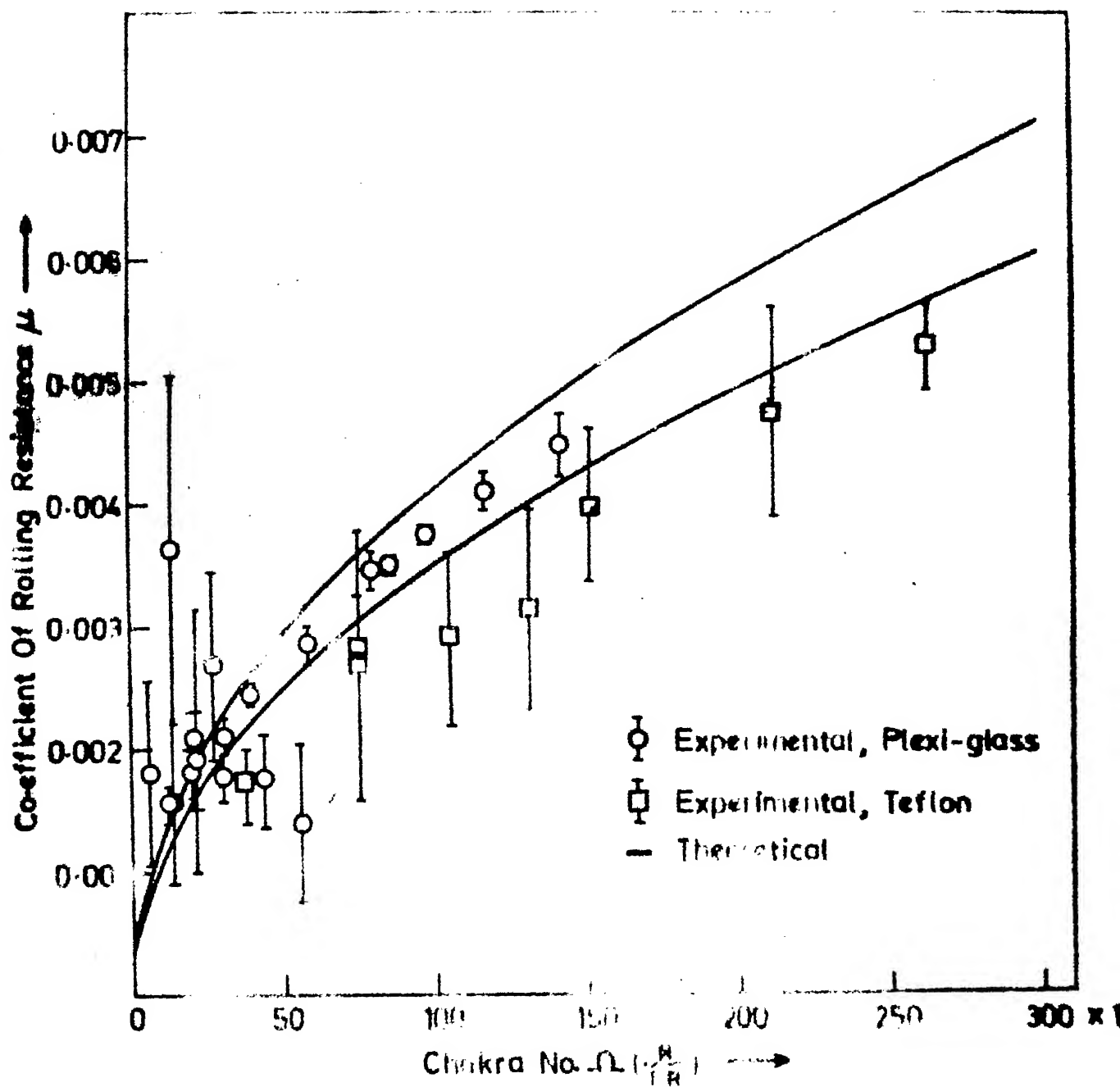


Fig.18  $\mu$  vs  $\Omega$  for Plexi-glass and Teflon wheels on Plexi-glass flat surface.

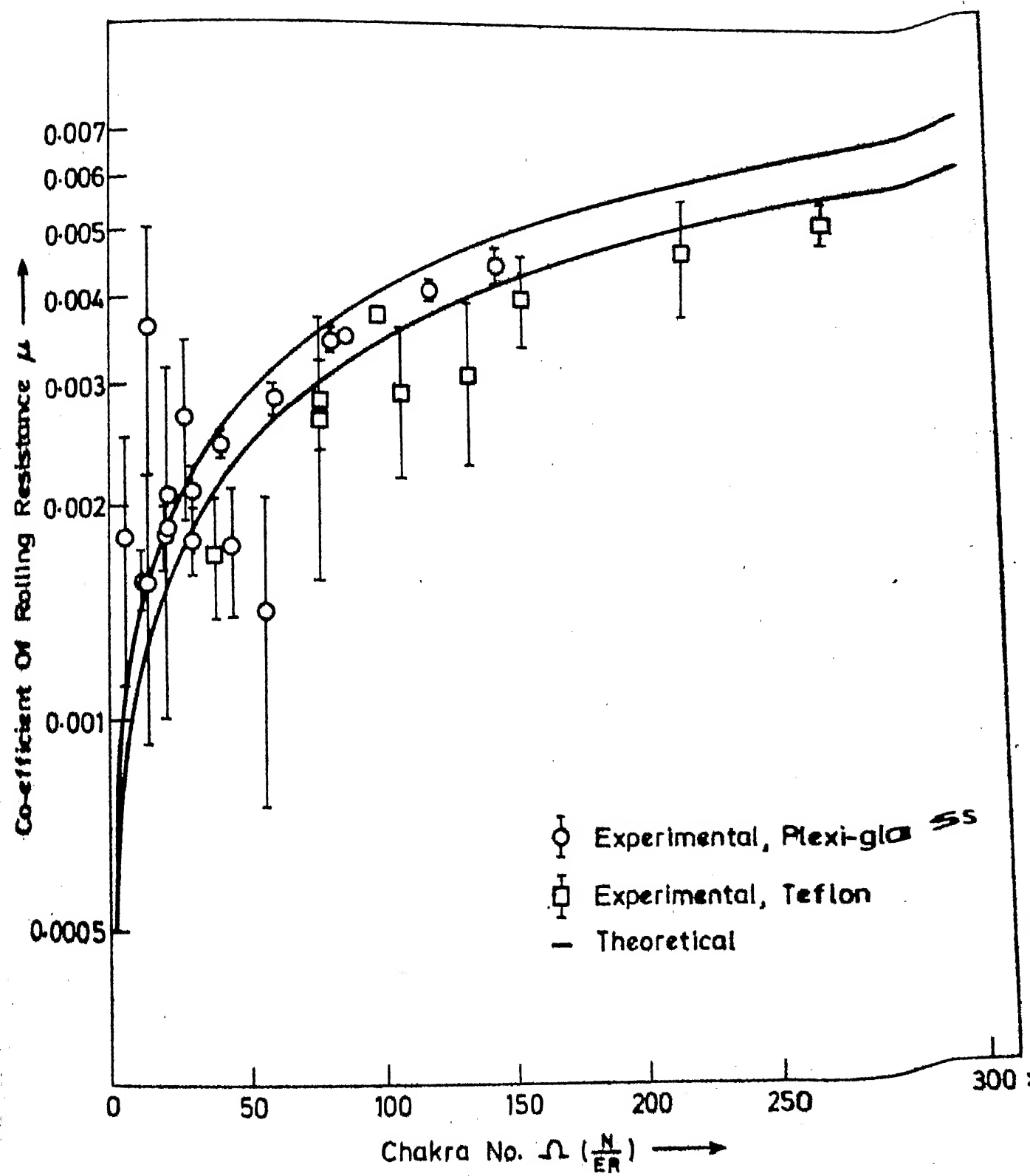


Fig.19  $\mu$  vs  $\Omega$  for Plexi-glass and Teflon wheels on Plexi-glass flat surface



Table 1 : Geometric Parameters, Material Constants and Chakra No. for Different Wheels

Set No.	Wheel No.	Materials	Radius of the wheel mm	Effective width mm	Mass kg.	Radius of Gyration mm	Load N/m.	CHAKRA NO. $\frac{N}{ER} \times 10^{-6}$
1.	1	Plexi-glass	88.33	13.96	2.396	49.10	1239.7	6.04
2.					5.464	46.70	2827.1	13.79
3.					9.394	46.98	4342.8	21.19
4.					10.732	45.47	5552.8	27.08
5.	2	Plexi-glass	84.16	9.6	2.727	47.19	2787.2	14.35
6.					5.795	49.75	5921.8	30.49
7.					8.325	46.57	8507.6	43.80
8.					10.664	45.13	10897.3	56.11
9.	3	Teflon	79.78	18.75	3.066	47.86	1600.0	37.77
10.			79.78		6.134	49.93	3200.0	75.54
11.			79.78		8.621	47.08	4498.3	106.19
12.			79.78		10.612	50.23	5537.4	132.01
13.	4	Plexi-glass	65.70	18.85	3.457	36.55	1799.0	11.99
14.					5.953	37.65	3097.8	20.65
15.	5	Plexi-glass	84.00	4.50	2.732	46.42	5954.7	30.72
16.					5.262	44.72	11471.2	59.18
17.					7.600	41.78	16569.1	85.48
18.					10.395	44.58	22661.1	116.90
19.					12.660	48.14	27597.7	142.37
20.	6	Plexi-glass	84.00	6.52	2.722	46.29	4094.8	21.12
21.					5.252	42.63	7902.2	40.76
22.					7.591	41.72	11420.7	58.92
23.					10.385	44.54	15625.3	80.61
24.					12.650	48.11	19032.4	93.18
25.	7	Teflon	79.00	9.36	3.036	47.47	3168.4	75.53

Table 2 : Co-efficient Rolling Resistance ' $\mu$ ' for Plexi-glass Wheels rolling on a Plexi-glass Flat Surface

S.No.	Wheel No.	$Q = \frac{N}{ER} \times 10^{-6}$	Experimental ' $\mu$ ' Standard deviation $\times 10^{-3}$	Mean $\times 10^{-3}$	Theoretical ' $\mu$ ' evaluated using simplified expression			Theoretical ' $\mu$ ' evaluated using accurate expression		
					Plane stress $\times 10^{-3}$	Plane strain $\times 10^{-3}$	Plane stress $\times 10^{-3}$	Plane stress $\times 10^{-3}$	Plane strain $\times 10^{-3}$	Plane strain $\times 10^{-3}$
1.	1	6.05	0.741	1.796	1.015	0.858	1.007	1.007	0.854	0.854
2.	1	13.79	0.635	1.565	1.533	1.296	1.516	1.516	1.287	1.287
3.	1	21.19	1.078	2.074	1.900	1.606	1.875	1.875	1.594	1.594
4.	1	27.09	0.787	2.676	2.148	1.816	2.117	2.117	1.800	1.800
5.	2	14.35	1.445	3.622	1.564	1.322	1.546	1.546	1.313	1.313
6.	2	30.49	0.204	1.777	2.279	1.927	2.244	2.244	1.909	1.909
7.	2	43.80	0.375	1.760	2.732	2.309	2.683	2.683	2.285	2.285
8.	2	56.11	0.642	1.400	3.092	2.614	3.030	3.030	2.582	2.582
9.	4	11.99	0.164	1.567	1.429	1.208	1.415	1.415	1.201	1.201
10.	4	20.65	0.191	1.801	1.876	1.586	1.852	1.852	1.573	1.573
11.	5	30.72	0.181	2.096	2.238	1.934	2.253	2.253	1.916	1.916
12.	5	59.18	0.155	2.866	3.176	2.684	3.111	3.111	2.651	2.651
13.	5	85.47	0.074	3.492	3.817	3.226	3.725	3.725	3.179	3.179
14.	5	116.90	0.134	4.117	4.463	3.773	4.34	4.34	3.708	3.708
15.	5	142.37	0.254	4.478	4.925	4.163	4.779	4.779	4.087	4.087
16.	6	21.12	0.152	1.834	1.897	1.604	1.872	1.872	1.591	1.591
17.	6	40.77	0.107	2.462	2.636	2.227	2.589	2.589	2.205	2.205
18.	6	58.92	0.127	2.854	3.169	2.678	3.104	3.104	2.646	2.646
19.	6	80.61	0.143	3.443	3.706	3.132	3.619	3.619	3.088	3.088
20.	6	98.18	0.069	3.758	4.090	3.457	3.987	3.987	3.404	3.404

Table 3: Co-efficient of Rolling Resistance ' $\mu$ ' for Teflon wheels Rolling on a Plexi-glass Flat Surface

S.No.	Wheel No.	CHAKRA NO. $Q = \frac{N}{ER} \times 10^{-6}$	Experimental ' $\mu$ '		Theoretical ' $\mu$ ' evaluated using simplified expression		Theoretical ' $\mu$ ' evaluated using accurate expression	
			Mean $\times 10^{-3}$	Standard deviation $\times 10^{-3}$	Plane stress $\times 10^{-3}$	Plane strain $\times 10^{-3}$	Plane stress $\times 10^{-3}$	Plane strain $\times 10^{-3}$
1.	3	37.77	1.714	0.336	2.537	2.144	2.494	2.123
2.	3	75.54	2.661	1.105	3.588	3.033	3.506	2.991
3.	3	106.19	2.907	0.721	4.254	3.595	4.142	3.538
4.	3	132.01	3.122	0.833	4.743	4.009	4.606	3.938
5.	7	75.53	2.838	0.432	3.588	3.033	3.506	2.991
6.	7	151.76	3.980	0.643	5.086	4.298	4.930	4.217
7.	7	211.48	4.721	0.851	6.003	5.074	5.792	1.963
8.	7	263.28	5.264	0.355	6.698	5.661	6.44	5.525

Table 4 : (a) Sample Calculations for Wheel No.5, Set No.16  
 $l_1 = 151.20$  mm     $l_2 = 146.20$  mm     $k = 42.72$  mm     $R = 34.00$  mm

Time $t_1$ $\mu$ sec.	Time $t_2$ $\mu$ sec.	Acceleration, $a$ , m/sec <sup>2</sup>	Co.ef., of rolling resistance ' $\mu$ '
1003559	1119112	0.018867263	0.002420665
1058983	1270021	0.023754608	0.003047711
925676	1030114	0.021898107	0.002809522
865469	950576	0.023018681	0.002953291
845989	932157	0.024615749	0.003158195
1155828	1427598	0.021990589	0.002821387
1163526	1446273	0.022118492	0.002837797
1177498	1460843	0.021474601	0.002755186
1200515	1538249	0.022566981	0.002895338
1200612	1537452	0.022529330	0.002890508
1300959	1536215	0.022454204	0.002880869
1205112	1539122	0.022211150	0.002849685
1207225	1549512	0.022413186	0.002875606
1138041	1393614	0.021901302	0.002809932
1148216	1400617	0.021421547	0.002748379
1142415	1398217	0.021876026	0.002806689
1178615	1453616	0.021053926	0.002701214
1116211	1336318	0.021245957	0.002725851
1118217	1341211	0.021313324	0.002734494
1148317	1399987	0.021380038	0.002743054
1149350	1400717	0.021315127	0.002734726
1251326	1650123	0.022181116	0.002850579
1267117	1684321	0.022040403	0.002827778
1216321	1590111	0.023065603	0.002959311
1178314	1505311	0.023249262	0.002982875
1116718	1370181	0.023077358	0.002960820
1138217	1380171	0.021371164	0.002741915
1241327	1649518	0.022950508	0.002944545
1244358	1647528	0.022663018	0.002907660
1247316	1650111	0.022516656	0.002888882
1058847	1276237	0.024188689	0.003103403
1081437	1321617	0.024295673	0.003117129
1062114	1283217	0.024239815	0.003109963
1078649	1316612	0.024325337	0.003120935
1094321	1345123	0.024168558	0.003100820
1010121	1130214	0.018996097	0.002437195
904067	1005778	0.022917182	0.002940269
951011	1076243	0.022834603	0.002929674
982454	1110413	0.021250859	0.002726480
1148116	1415217	0.022149520	0.002841778
1147471	1414161	0.022161795	0.002843353
1143333	1415168	0.022520079	0.002889321
1241329	1621621	0.022108829	0.002836558

Mean value of  $\mu = 0.002966543$ , Std. Deviation = 0.000154989  
 Co-efficient of Variation = 0.054068374

Table 4 : (b) Sample Calculations for Wheel No. 6, Set No. 24  
 $l_1 = 151.20 \text{ mm}$      $l_2 = 146.20 \text{ mm}$      $k = 48.11 \text{ mm}$      $R = 84.00 \text{ mm}$

Time $t_1$ $\mu \text{ sec.}$	Time $t_2$ $\mu \text{ sec.}$	Acceleration, $a, \text{ m/sec}^2$	Co. ef., of rolling resistance, ' $\mu$ '
1267899	1987099	0.028066259	0.003799620
1052177	1315266	0.027494504	0.003722215
1050266	1305459	0.027144313	0.003674806
1080506	1385208	0.027895143	0.003776454
1128472	1501546	0.027847850	0.003770051
1138989	1521232	0.027548834	0.003729571
1129568	1520209	0.028444278	0.003850796
1226959	1799820	0.027753038	0.003757216
1060762	1340526	0.027882849	0.003774790
970841	1152568	0.027214805	0.003684350
999811	1210562	0.027559358	0.003730995
996316	1200106	0.027258941	0.003690325
1138818	1670177	0.027736685	0.003755002
1146291	1560209	0.028227071	0.003821391
1133916	1513132	0.027745947	0.003756256
1120203	1500168	0.028637001	0.003876887
1111289	1456209	0.027778437	0.003760654
1200561	1697771	0.027483541	0.003720731
1374552	2694752	0.027398236	0.003709183
1144667	1550502	0.028049281	0.003797321
1146475	1543231	0.027621016	0.003739343
1190192	1661208	0.027376083	0.003706183
1255866	1970267	0.028636060	0.003876760
878547	1005767	0.028382370	0.003842415
854203	960001	0.027245550	0.003688512
893231	1020202	0.027143014	0.003674630
1233398	2020122	0.027472535	0.003719241
1236486	2024562	0.027372787	0.003705737
1227899	1801255	0.027711718	0.003751622
1229809	1810111	0.027749015	0.003756671
1228288	1810152	0.027863949	0.003772231
1234566	1851526	0.028197665	0.003817410
1220501	1840528	0.029042407	0.003931771
1139899	1531562	0.027838872	0.003768836
1133262	1525209	0.028260139	0.003825874
1234568	1852609	0.028217531	0.003820099
1294998	2064806	0.027353532	0.003703131
1300106	2100609	0.027464428	0.003718144
1301202	2105061	0.027448604	0.003716001
1105052	1430208	0.027297592	0.003695557
1141432	1490911	0.026139704	0.003538802
1156089	1590823	0.028310818	0.003832728
1146464	1560464	0.028219216	0.003820327

Mean value of  $\mu = 0.003757689$  , Sta. Deviation = 0.000069045  
 Co-efficient of Variation = 0.018374359

## CHAPTER-VI

### CONCLUSIONS, SCOPE AND FURTHER STUDY

#### Conslusions:

Rolling losses of a wheel rolling at low speeds on a flat surface are predicted by calculating elastic strain energy in both plane stress and plane strain modes. The co-efficient of rolling resistance is proportional to the square-root of a dimensionless group called Chakra Number  $Q = N/ER$ . In other words, the co-efficient of rolling resistance is

- (i) directly proportional to the square root of the normal load per unit width, of the wheel,
- (ii) inversely proportional to the square root of the radius of the wheel, and
- (iii) inversely proportional to the square root of the 'equivalent Young's modulus' of the wheel and flat surface.

Experiments are conducted using plexi-glass and Teflon wheels rolling on a plexi-glass surface. Special photo-diode system is developed to measure velocity of a

rolling wheel very accurately and conveniently. Also, ways are devised to increase load per unit width of a wheel by providing grooves in the centre of the wheel. Experimental results are in good agreement with theoretical predictions, specially at higher values of Chakra Number  $Q$  which gives coefficient of rolling friction as high as 0.006.

#### Scope and Further Study:

The aim with which present investigation started is due to the fact [13] that 25% of the fuel consumption in transportation goes to the rolling losses of tyres and if one improves the rolling resistance by 5% , there will be economy of fuel by 1% , that is, the ratio of improving the rolling resistance versus fuel economy is 5 to 1. This may be very important as the present day world is facing severe energy crisis.

By conducting the experiments in more controlled conditions such as keeping five photo-diodes instead of three, one can obtain time intervals  $t_1$  ,  $t_2$  ,  $t_3$  , and  $t_4$  and hence velocities  $V_1$  ,  $V_2$  ,  $V_3$  and  $V_4$  be evaluated. By observing these velocities, one can verify whether the acceleration is constant as assumed or not. And by keeping 'slip guages' (thin wedges of known slopes) under the ramp, one can control the velocity of the rolling wheel much better.

By conducting the experiment using different materials, one can further verify the relation obtained theoretically between  $\mu$  and  $\Omega$ . The next series of experiments may be conducted on Aluminium wheel rolling on Aluminium flat plate. One should use one of the high yield point alloys of Aluminium to avoid plastic flow. Then, the increase of Young's modulus,  $E$ , over plexi-glass is compensated by the increase in load per unit width,  $(N)$ .

For further checking the prediction of the theoretical formula, this experiment can be performed in a different manner, that is, by pulling the wheel at a constant speed using an electric motor <sup>and</sup> measuring the load by a load cell. One can also do this experiment using the inclined surfaces rather than flat one.



# REFERENCES

- [1] Coulomb, C.A., "Theories des Machines Simples", Me'moire de Mathematique et de Physique de l'Academic Royale 1785.
- [2] Bowden, F.P., and Tabor, D., "The Friction and Lubrication of Solids" Part II, Clarendon Press, Oxford Press, 1964, pp. 277-319.
- [3] Reynolds, O., "On Rolling Friction", Transactions of the Royal Society, Vol. 166, 1876, pp. 156-174.
- [4] Heathcote, H.L., "The Ball Bearings, in the Making, Under Test, and on Service", Proc. of Institution of Automobile Engineers, Vol.15, 1921, pp. 509-662.
- [5] Tomlinson, G.A., "A Molecular Theory of Friction", Philosophical Magazine, 57, Vol. 7, No. 46, June 1929, pp. 905-939.
- [6] Tabor, D., "The Mechanism of Rolling Friction II The Elastic Range", Proc. Roy. Soc., Vol. 229, Series A, 1955, pp. 193-220.
- [7] Holt, W.L., and Wormeley, P.L., "Power Losses in Automobile Tires", Technological Papers of the Bureau of Standards, 16(1922), pp. 451-461.
- [8] Drutowski, R.C., "Energy Losses of Balls Rolling on Plates", Trans. Amer. Soc. Mech. Engrs. 81, Series D, 1959, pp. 233-238.
- [9] Greenwood, J.A., Minshall, H., and Tabor, D., "Hysteresis Losses in Rolling and Sliding Friction", Proc. Roy. Soc.; Series A, V. 259, 1961, pp. 480-507.

- [10] S.J. Hasnain, "Energy Losses of Wheel Rolling Elastically on a Flat Surface", M. Tech. Thesis, I.I.T., Kanpur, 1983.
- [11] Smith, J.O., and Liu, C.K., "Stresses Due to Tangential and Normal Loads on Elastic Solids with Application to Some Contact Stress Problems", J. App. Mech., V 20, 1953, pp. 157-166.
- [12] Mckibben, E.G., and Davidson, J.B., "Effect of Outside and Cross Section Diameters on Rolling Resistance of Pneumatic Tires", Agric. Engr., V 21, 1940, pp. 57-53.
- [13] Clark, S.K., Dodge, R.N., Ganter, R.J., and Luchini, J.R., "Rolling Resistance of Pneumatic Tires", Interim Report, Contract DOT-TSC-316, University of Michigan, Ann. Arbor, Mich., July 1974.